Combining Hipparcos and Gaia data: Improved Astrometric Calculations With Orvara

Melvin Tham

Division of Astrophysics
Department of Physics
Lund University

2023-EXA216

Degree project of 15 higher education credits
January 2023

Supervisor: David Hobbs

Division of Astrophysics
Department of Physics
Box 43
SE-221 00 Lund
Sweden

Abstract

Hipparcos and Gaia are two missions intended to catalogue positions and motions of stellar objects. ORVARA is a computer program which aims to combine the data from these two missions to calculate Keplerian parameters for stellar systems. In practise, ORVARA can use any combination of radial velocity, relative astrometry and Hipparcos-Gaia data to generate results.

I present an investigation of ORVARA's approach to calculate these parameters as well as orbital parameters for AF Leporis b, Smethells 119 B, Gliese 105 C and Gliese 86 B. The results were produced using ORVARA and radial velocity data and relative astrometry data gathered from a variety of sources. The results in this thesis show the following: The exoplanet AF Leporis b was confirmed to exist with similar attributes as in other articles and the red dwarf companion Gliese 105 C was also confirmed to exist but with attributes that differ to some degree when compared to articles. For the two binary star systems, Gliese 86 and Smethells 119, the resulting parameters were quite different to those presented in other articles. The investigation of ORVARA is conducted by observing how the posterior parameters change when data is removed or changed. It turns out that ORVARA calculates accurate results when it is given all data that it can be given. From the results of this thesis one can conclude that there is a super Jupiter planet around AF Leporis, there is a red dwarf as the tertiary star in Gliese 105 and finally that Gliese 86 and Smethells 119 are binary systems of mass ratios 0.58 and 0.227. One can also conclude that ORVARA only generates accurate results if all sets of data are given.

Populärvetenskaplig beskrivning

Vi har alla fastnat med ögonen på en himmel full av stjärnor. Det är en helt naturlig reaktion att bli förtrollad av en stjärnklar natthimmel, vilket människor har blivit sedan urminnes tider. Ung eller gammal, klipsk eller enfaldig, alla har sin egen anledning till att låta ögonen dansa vals över natthimlen. Att veta vart stjärnor befinner sig vid olika tider har varit extremt viktigt för till exempel navigation och därmed skapades den äldsta versionen av astronomi: astrometri vilket är ämnet om kartläggandet av himlaobjekts position och rörelse. De tidigaste astronomerna var filosofer från antikens Grekland och Arabien och kartlade rörelsen och positionen hos många stjärnor som var synliga endast med ögonen. Här i Skåne är vi stolta över astronomen Tycho Brahe som använde instrument för att kunna kartlägga stjärnhimlen med mer precision än någonsin tidigare. Den moderna astrometrin använder sig av instrument som är så noggranna att de kan urskilja två stjärnor som kretsar runt varandra på andra sidan Vintergatan. Denna avhandling kommer hantera ett program som kombinerar data från två olika astrometriska uppdrag, Hipparcos och Gaia, i syfte att kunna räkna ut attribut av olika solsystem långt utanför vårt eget.

Hipparcos var en satellit som var aktiv under åren 1989-1993 och hade som uppdrag att kartlägga rörelserna och positionerna av ca 100 000 stjärnor vilket den kunde göra med en noggrannhet av 1 tusendels bågsekund, eller $2.8 \cdot 10^{-7}$ grader. Detta innebär att Hipparcos kunde mäta fel på positionen av objekt med ± 1 tusendels bågsekund. Detta uppdrag var sedan uppföljt av Gaia vilket också var en satellit som sköts upp i omloppsbana år 2013 med uppdraget att kartlägga position och rörelse av miljardtals himlaobjekt och Gaia är 100 gånger så noggrann i jämförelse med Hipparcos. Programmet som ska undersökas heter Orvara och det kan med hjälp av vilken kombination av data, däribland både Hipparcos- och Gaiadata, hitta olika egenskaper för alla möjliga typer av stjärnsystem. Till exempel ett stjärnsystem som har planeter runt sig eller ett stjärnsystem med två eller fler stjärnor i sig och så vidare. Skaparna av Orvara påstår att det kan hantera alla möjliga olika kombinationer av datatyper och att den kan hantera många olika typer av stjärnsystem.

I denna avhandling kommer jag att, med hjälp av Orvara, generera resultat för följande stjärnsystem: AF Leporis, som påstås ha en planet ungefär 4 gånger så massiv som Jupiter runt sig. Gliese 105, som påstås vara ett trinärt stjärnsystem där en av stjärnorna endast ska ha ungefär 1% av solens massa. De två sista systemen påstås vara binära stjärnsystem vid namn Gliese 86 och Smethells 119. Orvara kommer även att undersökas för att se dess svagheter och styrkor samt att undersöka hur programmet prioriterar de olika typerna av data och hur väl det fungerar utan vissa typer av data.

Contents

Chapter 1

Introduction

Astrometry is the science of mapping the skies, cataloguing the motions and positions of astronomical objects. Getting accurate measurements of objects' positions and motions is vital when for example testing theoretical relationships about movements of bodies, or just to know where each body is at a certain time such that they can be observed. It is one of the oldest branches of astronomy and today we are using highly accurate instruments to get precise measurements of the positions and motions of cosmic objects.

Hipparcos was a satellite in operation between 1989 and 1993. It was tasked with determining the positions, parallaxes and annual proper motions with an accuracy of 1 milliarcsecond (mas) for 120 000 stars in our galaxy. This was the first satellite tasked with conducting astrometric measurements. The data became available after the mission ended with the measurements and their corresponding epoch[1] measurements, allowing it to be used for calculations when, for example, finding exoplanets and their attributes (Perryman 2018). Hipparcos was followed up by the Gaia mission which was launched in 2013 and the final epoch astrometry data will be released in 2025. This mission maps 1-2 billion, not only stars but also quasars, asteroids and more. This mission is expected to have an accuracy on the positions of the stars of about 20-25 μas at a visual magnitude of 15. Data from the mission has been released at regular intervals with the latest being released in 2022 and the final release of the astrometric parameters being scheduled for 2030. Before this however, the released data cannot be used for any astrometric calculations about the internal properties of stellar systems which requires epoch data (Perryman 2018).

In 2021, a computer program known as Orvara was released which aimed to combine Hipparcos, Gaia, radial velocity and relative astrometry data in order to get accurate results for the orbital parameters of stellar systems. In the article Brandt et al. (2021), the authors claim that the program can achieve good results much quicker than any rivaling program which is a great improvement to the astrometry that can be done before the full Gaia data is released. This means that, at least until the epoch Gaia data is released,

[1] Individual time dependent measurements.

Orvara has a good chance to become an established program within the astronomic community and thus it is important to investigate the integrity of this program. Furthermore, the same fast and accurate algorithm used in Orvara can potentially be used when the full epoch data for Gaia is released. In this project, the program will be investigated in the following manner: Results will be generated for a diagnostic system without certain sets of data to observe how the results change based on what data is available for Orvara. To investigate how Hipparcos data is used, results will also be generated with Hipparcos data belonging to a different system.

The main objective of this thesis is to investigate the properties of four specific systems. According to Franson et al. (2023), AF Leporis has a super Jupiter exoplanet. Feng et al. (2021) states that Gliese 105 has a brown dwarf companion, making it a trinary star system and according to the GCVS catalogue (Samus et al. 2009), the red dwarf has a much smaller semi-major axis than Gliese 105 B, about 20 a.u versus about 1200 a.u. This means that Gliese 105 C orbits A and B orbits them both. Gliese 86 is a binary star system according to Zeng et al. (2022) and Smethells 119 is also a binary star system according to Bonavita et al. (2022). These systems are going to be investigated using Orvara to confirm, or to put into question, the existence of these companions. If they are confirmed to exist, new attributes of the companions and their orbits, such as mass and orbital period, will be proposed. The aforementioned systems are used in this thesis since all sets of data Orvara can use were available. It will become evident later in the thesis why it is necessary to include all types of data. When it comes to the two systems with a larger difference in mass, Gliese 105 A-C and AF Leporis, they will also be investigated to see how Orvara handles systems of smaller astrometric signature. It is always important to use new techniques and programs to improve the calculated properties of stellar systems which is why this part of the thesis is important for the further improvement of astronomical data for stars in the galaxy. The results from a fifth system, HD 114082, will also be included where the fit failed since it is important to show that a fit can fail and how it might look when it fails.

This thesis is split into two major parts: Generating results for four stellar systems of different kinds and a part where Orvara is investigated. The general goal of this thesis is thus to not only investigate the four systems and generate results for the orbital parameters of their companions, but also to investigate Orvara as a program. The layout of the chapters in the thesis are the following: In chapter 2, it is described how Orvara works and how the program will be tested. Chapter 3 discloses the results where all plots for Gliese 86 are presented and the plots for the other systems are in the appendix. chapter 3 also discloses the posterior parameters for the systems and also the results from the tests. Chapter 4 is the discussion and conclusions where the results are compared to the literature, the plots are discussed and lastly the data sets are also discussed. Appendix A shows the rest of the figures that were not presented in chapter 3 and appendix B Shows a table of the settings used for all systems. In table 1.1, the four investigated systems are listed with some of their attributes. Table 1.2 summarizes some attributes for the additional systems used during the testing of Orvara.

Table 1.1: Table describes some attributes of the stellar systems that are investigated in this thesis. The values are taken from the results of this thesis.

System	**AF Leporis**	**Gliese 105 (A-C)**	**Gliese 86**	**Smethells 119**
System configuration	Single exoplanet	Trinary star	Binary star + exoplanet	Binary star
Distance (pc)	26.843	7.229	10.761	23.527
Mass ratio M_{sec}/M_{pri}	0.00297	0.083	0.58	0.227
Orbital Period (yrs)	20.7	47.3	228	20.0
Semi-major axis (A.U)	8.00	12.6	40.3	7.33

Table 1.2: Table summarizing some attributes for systems used in this thesis during the testing of Orvara.

System	**HIP 95319**	**HIP 85653**	**HD 114082**
System configuration	Single exoplanet	Binary	Single exoplanet
Distance (pc)	15.6	21.7	95.06
Mass ratio M_{sec}/M_{pri}	0.037	0.85	0.0053
Orbital period	∼300 yr	238 yr	109 days
Semi-major axis	33 A.U	60 A.U	0.51 A.U
Reference	Brandt et al. (2019)	Hirsch et al. (2019)	Zakhozhay et al. (2022)

1.1 Theory

The objective of Orvara is to determine 16 parameters to the stellar system of the users choice. 10 of these parameters are fitted using Markov chain Monte Carlo (MCMC) and from these parameters, the last 6 can be derived (Brandt et al. 2021). The fitted parameters are the following: radial velocity jitter (essentially noise), mass of the primary star, mass of the companion, semi-major axis (in A.U), $\sqrt{e}\sin(\omega)$, $\sqrt{e}\cos(\omega)$, inclination, mean longitude with the reference epoch at 1 January 2010, 00:00 UT, ascending node and parallax. The 6 derived parameters are: The orbital period, the argument of periastron, eccentricity, semi-major axis (mas), time of periastron and the mass ratio between the bodies (Brandt et al. 2021). These parameters are described by posterior and prior distributions which in turn are described by Bayes theorem as described below. However, since this system is

very complicated, one can approximate this posterior using the Markov chain Monte Carlo method as described below.

1.1.1 Orbital parameters

A Keplerian elliptic orbit can be described by 6 parameters. The shape of the ellipse is described by the semi-major axis (a) and the eccentricity (e), which are the half of the major axis of the ellipse and how elongated the ellipse is, respectively. The inclination (i) and the longitude of the ascending node (Ω) describe the orientation of the orbit in the reference plane (see figure 1.1). The reference plane is face on to the observer as shown in figure 1.1 and i, Ω are the angle of the orbit to the reference plane and the angle of rotation of the orbit based on the reference direction respectively (Perryman 2018). The last two parameters are the argument periastron (ω) which describes the orientation of the ellipse and is the angle between the reference plane and the tip of the ellipse and the true anomaly ($v(t)$) describes the position of the orbiting body in the ellipse.

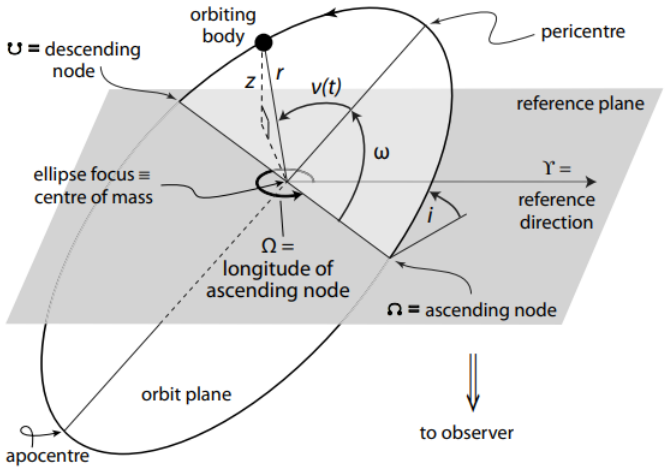

Figure 1.1: Example of an orbit where four of the six Keplerian orbital parameters are displayed. These four parameters are: the inclination i, ω is the argument of periastron, $v(t)$ is the true anomaly and Ω is the longitude of the ascending node (Perryman 2018).

Thiele-Innes parameters

ORVARA uses the so called Thiele-Innes parameters which separate the linear geometric and non linear dynamical parameters in the orbit. They are formulated in the following way (Brandt et al. 2021):

$$A = \cos\omega\cos\Omega - \sin\Omega\sin\omega\cos i$$

$$B = \sin\Omega\cos\omega + \cos\Omega\sin\omega\cos i$$

$$F = -(\cos\Omega \sin\omega + \sin\Omega \cos\omega \cos i)$$

$$G = -\sin\Omega \sin\omega + \cos\omega \cos\Omega \cos i$$

In ORVARA, these are used to calculate the projected offsets of the companion with respect to the primary star in declination and right ascension as follows (Brandt et al. 2021):

$$\Delta\delta = a(AX + FY)$$

$$\Delta\alpha* = a(BX + GY)$$

where $\Delta\alpha* = \Delta(\alpha \cos\delta)$. The elliptic rectangular coordinates depicting the projected offset between the two bodies are: $X = \cos E - e$ and $Y = \sin E\sqrt{1-e^2}$. In these equations, E is the eccentric anomaly and e is the eccentricity. The eccentric anomaly and eccentricity are related through Kepler's equation as follows:

$$E - e\sin(E) = 2\pi\frac{t - T_0}{P}$$

where t is an arbitrary time, T_0 is the time of periastron (the time at which the body is at the periastron), and lastly, P is the orbital period.

Another important angle when using ORVARA is the position angle (θ) which is used in the relative astrometry data for binary systems. This angle is defined as follows: draw a line from the primary to the secondary stars and another line from the primary star to the north celestial pole. The angle that these two lines create between each other is then the position angle which is positive if the secondary star is due east of the primary star (Altena & Horch 2013). A diagram of this can be seen in figure 1.2. The position angle can be expressed in a mathematical relation as

$$\tan(\theta - \Omega) = \pm\tan(v + \omega)\cos(i) \tag{1.1}$$

where v is the true anomaly of the orbit.

Astrometric signature

The astrometric signature of a star tells us how large the orbital movements of the star will be on the night sky. This signature gives a good indication of how much the planet or star affect the movements of the parent star and it is given by:

$$\alpha = \frac{M_p}{M_* + M_p}a \approx \frac{M_p}{M_*}a \tag{1.2}$$

where M_p and M_* are the masses of the orbiting body and the star respectively and a is the semi-major axis. In the above equation, the approximation can only be done in the case when the difference in mass, between the central body and the orbiting body, is large.

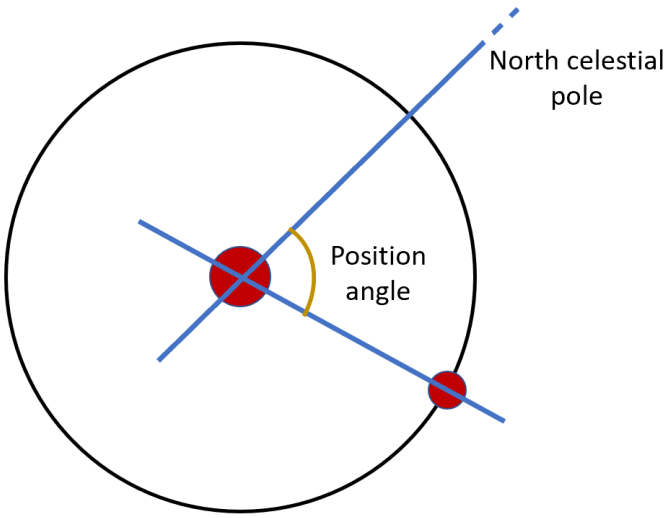

Figure 1.2: Diagram showing an illustration of how to calculate the position angle of a binary star system. The position angle is positive or negative according to equation 1.1.

Proper motion

In astrometry, proper motion is a common concept which is present in both Gaia and Hipparcos data. Proper motion is, unlike what the name conveys, not the actual motion of the stellar body in space. It is instead the angular motion of the object on the sky and is usually expressed in mas/yr. If the proper motion of the secondary star is not included in the Gaia/Hipparcos data, this can be calculated using the following relationship which is in the frame of the systems barycenter (Brandt et al. 2021):

$$\mu_B = -\mu_A \left(\frac{M_A}{M_B}\right) \tag{1.3}$$

Where μ_B is the proper motion of the companion, μ_A is the proper motion of the primary star, M_A and M_B are the mass of the primary star and the companion respectively.

1.1.2 Bayes theorem

Bayes theorem is a useful mathematical theorem in many fields when one has to calculate the posterior probability $P(A_j|B)$. It states the following: if $A_1, A_2, ..., A_k$ are k mutually exclusive to one another and where their individual probabilities are greater than zero then, for another event B with probability greater than zero, the following holds

$$P(A_j|B) = \frac{P(B|A_j)P(A_j)}{\sum_{i=1}^{k} P(B|A_i)P(A_i)}$$

for $1 \leq j \leq k$. In the case where A is continuous, the summation in the denominator in the above equation can be changed to an integral over A (Devore 2000). If this integral is

complicated or impossible to solve analytically, it can be approximated using the methods presented below.

1.1.3 Markov chain Monte Carlo

ORVARA utalizes Markov chain Monte Carlo (MCMC) methods using the PYTHON package PTEMCEE (Foreman-Mackey et al. 2013; Vousden et al. 2016) in order to fit parameters to the Keplerian orbital equations. The reason for why this method was chosen is because it is the standard and is the most efficient. MCMC is a combination of two methods which are explained below:

Monte Carlo sampling

If one has a complicated integral which has a very difficult or non-existent analytical solution, one can use Monte Carlo sampling to approximate the answer. Say we have a complicated integral which can be split up as follows

$$s = \int_a^b p(x)f(x)dx$$

where $f(x)$ is a function and $p(x)$ is a probability density function defined between a and b. If we now take a large number (n) of random points from $p(x)$, the integral can be estimated as:

$$s \approx \frac{1}{n}\sum_{i=1}^{n} f(x_i)$$

where x_i are the resulting variables from this random drawing. This equation is known as Monte Carlo integration (Walsh 2004).

Markov Chains

Intuitively, Markov chains are chains of states where the transition probabilities of the current state does not depend on the previous state, only the current state. An example for this could be that the road is wet, thus your car has a probability to slip and this does not depend on why the road is wet such as rain or hose etc. Mathematically, the Markov property is formulated as (Walsh 2004)

$$p(X_{t+1} = s_j | X_0 = s_k, ..., X_t = s_i) = p(X_{t+1} = s_j | X_t = s_i)$$

where $p(A|B)$ means the probability of A given B, X_t is a random value from a variable. What this equation says is that the probability that $X_{t+1} = s_j$ given all previous values is equal to the probability that $X_{t+1} = s_j$ given that the previous value $X_t = s_i$. In short, if a process exhibits this Markov property, it is a Markov chain (Walsh 2004).

Stationary distribution

A Markov chain can reach a state called stationary distribution which is when we have states with individual probability distributions s_i and a transition probability matrix Q which tells us the probability for states to transition from one to the next. This means that we have $s_{i+1} = s_i Q$ and if we keep multiplying these together for many iterations, s will stop changing and we have reached whats known as a stationary distribution. This distribution does not depend on the initial state and as such, it will always be reached no matter from which state we begin. In short, stationary distribution shows the probability of being in a given state at a given time (Walsh 2004).

MCMC

If we now combine the aforementioned topics, we achieve whats known as a Markov chain Monte Carlo. In PTEMCEE, the method for calculating the MCMC chain is a modified version of the Metropolis-Hastings algorithm which, in short, uses the following procedure (Foreman-Mackey et al. 2013):

1. Sample a proposal position Y from the transition distribution $Q(Y|X(t))$.

2. This proposed position has the following probability to be accepted:

$$\frac{p(Y)Q(X(t)|Y)}{p(X(t))Q(Y|X(t))}$$

3. If it is accepted: $X(t+1) = Y$, else: $X(t+1) = X(t)$.

This procedure is then iterated until the chain reaches a stationary distribution.

Burn-in is a concept used in ORVARA in which the chain is allowed to move towards the stationary distribution for a number of steps that are then thrown away for the chain to continue converging from that point. This can be done since, as stated above, the transition probability for the state at $t+1$ is not dependent on the transition probability of the state at t. This means that one can safely ignore the states before the chain has started converging (Walsh 2004).

Chapter 2

Method

2.1 Orvara

Orvara's method to solving the orbital parameters is described in detail in Brandt et al. (2021). The main author behind Orvara, Timothy D. Brandt, has also released a combined Hipparcos-Gaia data set (HGCA) (Brandt 2021) which is a cross calibration of the two sets. The methods used improved precision by a factor of 3 over the last HGCA cross calibration (Brandt 2021). To get a good fit, there are also two more required sets of data: Radial velocity data and relative astrometry data. Radial velocity data consists of 3 required types of data: time, radial velocity and the radial velocity error. The relative astrometry data consists of 5 types of required data: time, angular separation, angular separation error, position angle and position angle error. These need to be gathered from separate sources other than Gaia or Hipparcos. If the user wants to use epoch astrometry, the program also needs to supplied with three more files: The original reduction of the Hipparcos data, the Floor van Leeuwen reduction of the Hipparcos data and finally, the observational Gaia epochs and scan angles that are available. This data is, however, downloaded automatically by the program if they are not supplied manually. The two Hipparcos reductions are then combined in a 40/60 split as described in both Brandt et al. (2021) and Brandt (2021). If one does not want to use the HGCA data or the star does not exist in that set, then one needs to supply a parallax and a parallax error to the program (Brandt et al. 2021).

In order for different data sets to be used in calculations together as in the HGCA data set, they need to encompass the same epochs and be cross-calibrated. In HGCA, this is done by propagating positions of Gaia to the middle of the Hipparcos epochs in order to minimize uncertainty on the positions and also removes any covariance between position and proper motion. The two data sets also need to be calibrated to one another such that they can function as a single data set. This is done by only calibrating on stars that have a very low proper motion in both data sets since the movements are linear and simple. This leaves us with 87 000 stars that can be used for calibration. To avoid overfitting the

calibration to these stars, in Brandt (2021), 10% of the stars are used as validation to see how well the calibration turned out. If the individual Hipparcos and Gaia data files are used then these are treated using the same calibration and propagation as the HGCA data (Brandt 2021).

Orvara determines the aforementioned 16 parameters for the system, 6 of which are the Keplerian orbital elements. This is done by fitting a number of Keplerian orbits to an arbitrary combination of data, then it handles the full motion of the object as a linear combination of these Keplerian orbits. Orvara also uses a program called "hundred thousand orbit fitter" (Htof) (Brandt et al. 2021) which uses known Hipparcos- and predicted Gaia[1] observation times and scan angles to solve for the best fitting proper motion and position relative to the barycenter. These values are then compared to the respective values in the HGCA catalogue. After this, since we are only interested in the movement of the star and its companion(s) by themselves, the RV zero point, the parallax and the barycenter proper motion are marginalized out. Orvara then performs MCMC, using Ptemcee, to fit the rest of the Keplerian orbital parameters. In order to reduce confusion regarding the data used in this thesis, figure 2.1 has been created which gives a more graphical representation of how they are used or what information they contribute to the calculations.

If a system has more than one companion the aforementioned methods produce much worse results. This is because Keplerian orbits only describe two-body systems. In order to solve the orbit of companion i, Orvara utilizes some approximations. First, the star's motion is approximated using a superposition of the Keplerian orbits of the companions. Then, the star and the companion $\neq i$ are approximated to be the same body, combining the mass and moving the orbits closer to each other. When it comes to relative astrometry, all companions orbiting outside of companion i are ignored. The relative astrometry is then computed for companion i and the barycenter of all companions orbiting inside of companion i. And lastly, an offset is added to companion i which is due to the inner companions. Using these approximations should allow Orvara to produce accurate results for any companion in a multi-body system.

The program is controlled through two commands, fit_orbit and plot_orbit which calculates the Keplerian parameters using MCMC and plots the results respectively. These commands are customized using a configuration file of which I will go through the more important settings (An example of a configuration file can be seen in the tutorial file [2]) and a table of the file can also be seen in Brandt et al. (2021). The file begins with directories to all the different kinds of data you would like to use in the calculations.

After this comes the MCMC settings which are very important. `ntemps` is a variable stating how many temperatures in the parallel tempering chain (it is essentially a method

[1] From: `https://gaia.esac.esa.int/gost/`

[2] `https://github.com/t-brandt/orvara/blob/master/Tutorial.ipynb`

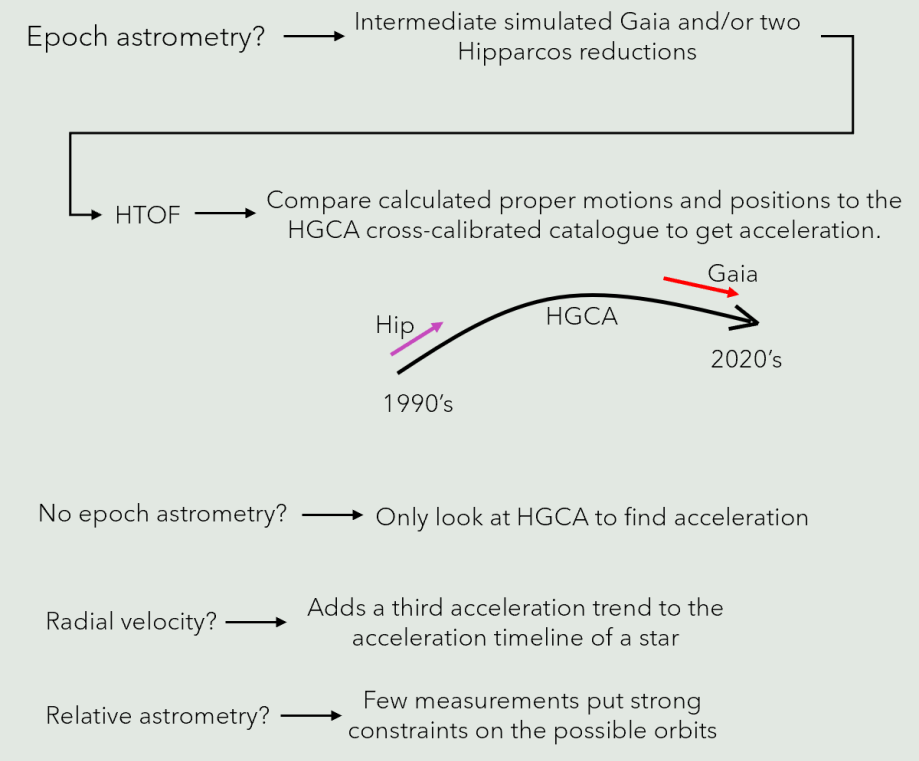

Figure 2.1: Simplified representation of the data sets and what information they contribute with to the calculations and/or how they are used in ORVARA. The HGCA (Hipparcos Gaia Catalogue of Accelerations) is a cross validated Hipparcos-Gaia combined data set (Brandt 2021) and HTOF (Hundred Thousand Orbit Fitter) is a program that fits intermediate astrometric data to astrometric parameters of any system (Brandt et al. 2021).

to create diversity among the chains to accurately and quickly find the minimum). Then you need to define the number of walkers that will each have `ntemps` number of chains using the variable `nwalkers`. Next, the number of planets/companions need to be defined using the variable `nplanets`, and the varable `nstep` is the number of steps every chain will take. The next variable is `thin` which determines that only every `thin`-th step will be kept (thinning is simply put a way to reduce correlation in the simulations). The next important variable is `use_epoch_astrometry` which is either True or False and defines whether to use the two Hipparcos reductions, the individual Gaia data and HGCA if True or only HGCA if False.

Next comes the priors settings where you can input any known data about the system such as parallax or primary star mass. For all the systems, the priors were left for ORVARA to guess except for the primary mass which was given. Initial values for the walkers are left up to ORVARA to decide. This is done by drawing the starting values for each of the walker from a normal or a lognormal distribution as described in Brandt et al. (2021). The

primary mass can be set in the `mpri` which then is the mean of a gaussian prior on the primary mass. The parallax and its error is required if you want to ignore the HGCA data set. The next section after this is the secondary Gaia which can be used if the secondary star exists in the Gaia data set. The next section is the plotting section where you can specify parameters that determine how the results are created or how plots will look. The most important of these variables are the following. The variable `burnin` defines the burn in for the chain and the variable `iplanet` defines which companion you want to plot, if there are more than one companion in the system. The rest of the variables simply defines attributes of the plots such as `num_orbits` which states the amount of orbits, randomly drawn from the posterior distribution, to be plotted. The configuration file variables used for each system can be found in table B.1.

2.2 Testing ORVARA

In order to test how well ORVARA works with different combinations of data, I chose to use AF Lep as a diagnostic system. AF Lep is a good system for this since it contains one exoplanet around a single star. This means that its astrometric signature will be small meaning that any changes to the data should lead to large differences in the results. A range of different combinations of data were attempted and this was done as follows: First, the two individual Hipparcos data files containing the two reductions were changed to the data of HIP 10138 (aka Gliese 86) and HIP 95319 for two separate runs. A summary of these systems' attributes can be found in table 1.2. After this, the Hipparcos files were changed back and simulated Gaia data was changed to HIP 85653 a summary of the attributes of which can slo be found in table 1.2. Then a run was conducted without the HGCA data and with a parallax of 37.25 was provided. Next, results were generated with correct Hipparcos data, Gaia data and HGCA data but without the relative astrometry and radial velocity data. The last diagnostic tests were to run ORVARA with only HGCA data and then with all data but with `use_epoch_astrometry` set to False. For all the tests, the following important settings remained unchanged: `mpri` was set to 1.2 solar masses, 100 walkers, `nplanets`=1, 20000 steps, `thin`=50 and `burnin`=100. The rest of the settings are the same as for AF LEP in table B.1 and were not changed for any of the diagnostic runs.

Chapter 3

Results

3.1 Production of results

In order to see if each system has a companion and if so determine its attributes. The following plots were produced: astrometric orbit plot, position angle plot, radial velocity (RV) plots, separation plot, proper motion plots, diagnostic plot and correlation plot. The different systems were chosen on the basis of observing how Orvara handles producing results for different mass ratios and attributes. Smethells 119 and Gliese 86 are binary stars with similar masses between their respective primary and secondary stars. AF Leporis is a exoplanet system which means that the mass will be very low. And for the last system, the trinary Gliese 105, where the small red dwarf is investigated, I wanted to investigate how the program handles when a much more massive star, compared to the red dwarf, is affecting the motion of the primary star. The following subsections outline using which settings and data were used to produce results for each system.

3.1.1 Gliese 86

The first system I produced results for was the binary Gliese 86 A-B. I used Radial velocity data from Figueira et al. (2010) consisting of 24 data points that are CRIRES data with an approximate uncertainty of $\pm 8 - 18$ m/s and relative astrometry data compiled in Zeng et al. (2022) consisting of 8 data points from various sources where the angular separations and the position angles have an approximate uncertainty of $\pm 1\%$ and $\pm 0.5\%$ respectively. The important settings used for this system were 100 walkers, `nplanets`=2, 20000 steps and `thin` to 50. `mpri` was set to 0.8 solar masses, `burnin`=50 steps and `numorbits`=50.

3.1.2 Smethells 119

The first system I produced results for was Smethells 119 where I used 66 radial velocity data points from HARPS as presented in Biller et al. (2022) and of approximate uncertainty $\pm 5 - 9$ m/s and 1 relative astrometry data point from Bonavita et al. (2022). For the relative

astrometry, the separation angle between Smethells 119 A-B was stated and the position angle was calculated using equation 1.1 with an uncertainty of ±1%. For this system I used 100 walkers, set `nplanets`=1, 20000 steps and `thin` to 50. `mpri` was set to 0.8 solar masses, `burnin`=110 steps and `numorbits`=50.

3.1.3 AF Leporis

The third system I produced results for was the exoplanet in AF Leporis. The radial velocity data was taken from the LCES HIRES/Keck radial velocity survey (Butler et al. 2017) consisting of 20 data points of approximate uncertainty $\pm 50 - 70$ m/s and the relative astrometry data was taken from IFS as presented in Mesa et al. (2023) consisting of 2 data points with approximate uncertainty of ±1% for both position angle and angular separation. For this system I used 100 walkers, set `nplanets`=1, 20000 steps and `thin` to 50. `mpri` was set to 1.2 solar masses, `burnin`=100 steps and `numorbits`=500.

3.1.4 Gliese 105 (C)

The final system is a trinary system consisting of two larger stars and a small red dwarf called Gliese 105. For this system, I generated results for the smaller red dwarf (Gl 105 A-C system) using 115 radial velocity data points from LCES HIRES/Keck radial velocity survey (Butler et al. 2017) with an approximate uncertainty of ±1.2 m/s and 3 relative astrometry data points from Golimowski et al. (2000) with an approximate uncertainty of ±1% for both position angle and angular separation. The important settings used for this system were as follows: 100 walkers, set `nplanets`=2, 20000 steps and `thin` to 50. `mpri` was set to 0.74 solar masses, `burnin`=100 steps and `numorbits`=500.

3.1.5 Extra: HD 114082

A fifth system known as HD 114082 is also included in this thesis as an example of a failed fit. according to Zakhozhay et al. (2022) it is an sun-like star with a hot Jovian planet in its orbit that should be around eight Jupiter masses. For the fit, I used a total of 82 radial velocity data points presented in Zakhozhay et al. (2022) where 64 of them are FEROS doppler measurements with an approximate uncertainty of $\pm 50 - 100$ m/s and 18 are HARPS doppler measurements with an approximate uncertainty of $\pm 3 - 7$ m/s. No relative astrometry data was found for this system since I was unable to find it. The settings used for this fit were the same as for AF Leporis with the difference of `burnin`=50 and `mpri`=1.47 solar masses. The posterior parameters of the fit are presented in the diagnostic results section below and its plots are presented in the appendix. This is done in order to avoid confusion and to avoid mixing the results from this system with the much more accurate results of the other four systems.

3.2 Gliese 86 plots

In order to conserve space in this thesis, only all plots from Gliese 86 are included in the results. The same plots for the rest of the systems can be found in the appendix. However, a detail which is also discussed later in the discussion section is that often Orvara will remove or change elements in the plots making them harder to decipher. In the plots presented here, figure 3.1 right does not show the data points which are shown in the left plot. This is because the x-axis on the left plot is only supposed to span 13 days in January 2008. In the six plots presented below, figures 3.2 and 3.1 show that the different fits have low spread and that the O-C plots stay close to the center. This means that there is a clear general solution that the chains have converged to. This can also be seen in figure 3.3 where the large majority of the chains have converged in the same region and figure A.1 where an overview of the chains is given. In both of these plots it is clear that the chains have mostly converged except for a smaller region which broke off at the end suggesting that longer computational time would have been necessary. The proper motion plots in figure 3.4 show that the fits are less in agreement with one another and in the O-C plots, the fits are not close to the center. This is most likely due to that the measurements are far apart in time from one another.

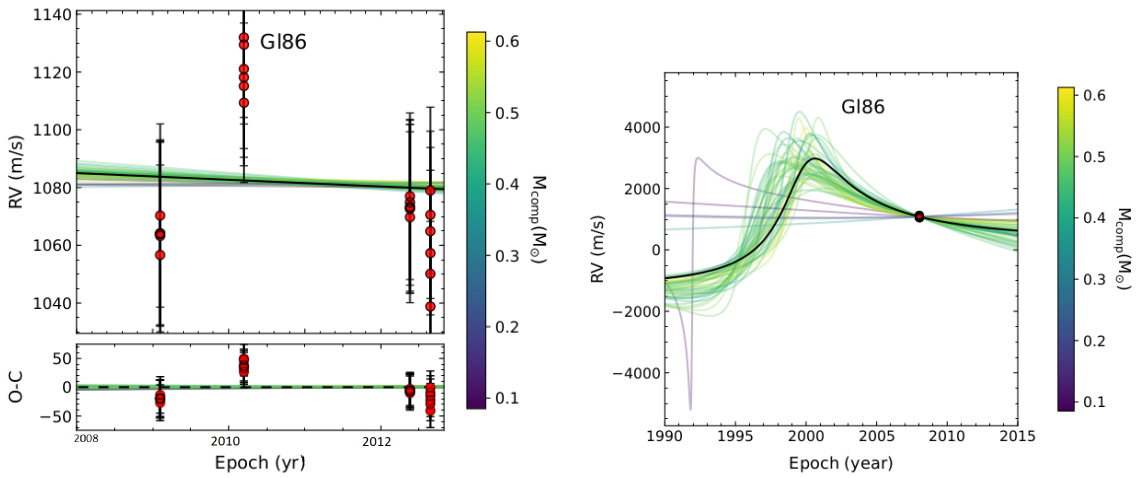

Figure 3.1: Radial velocity plots that show the radial velocity data plotted against the epoch with their accompanying fits randomly drawn from the posterior distribution coloured according to secondary mass. The two plots show the same thing just different levels of zoom. O-C stands for observed minus calculated and is included on the left plot.

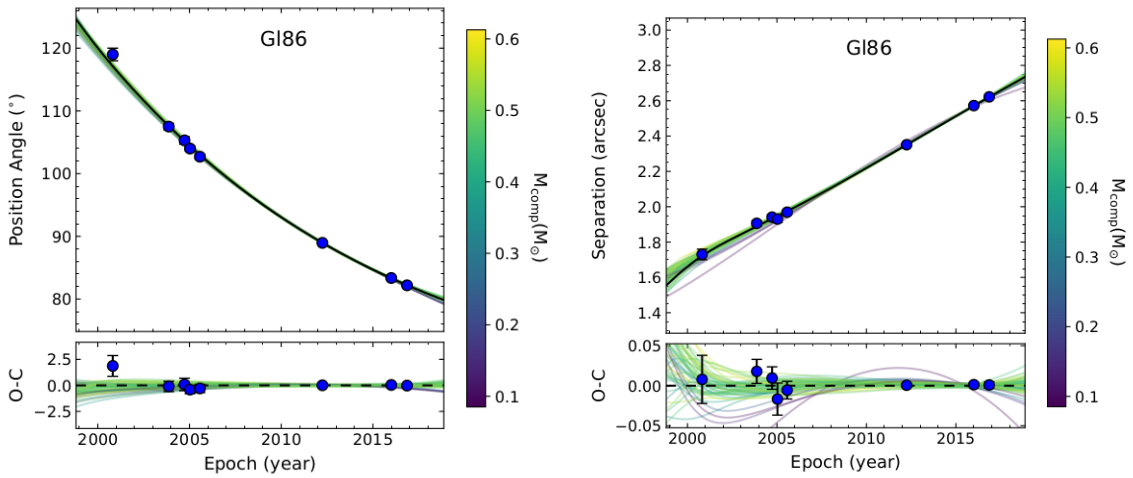

Figure 3.2: Left: Position angle plotted against epoch. Right: the angular separation plotted against epoch. The data points in both plots is the relative astrometry data. Random fits from the posterior distribution are also plotted and coloured according to secondary mass with the most probable fit in black. Lastly, observed minus calculated plots are also included.

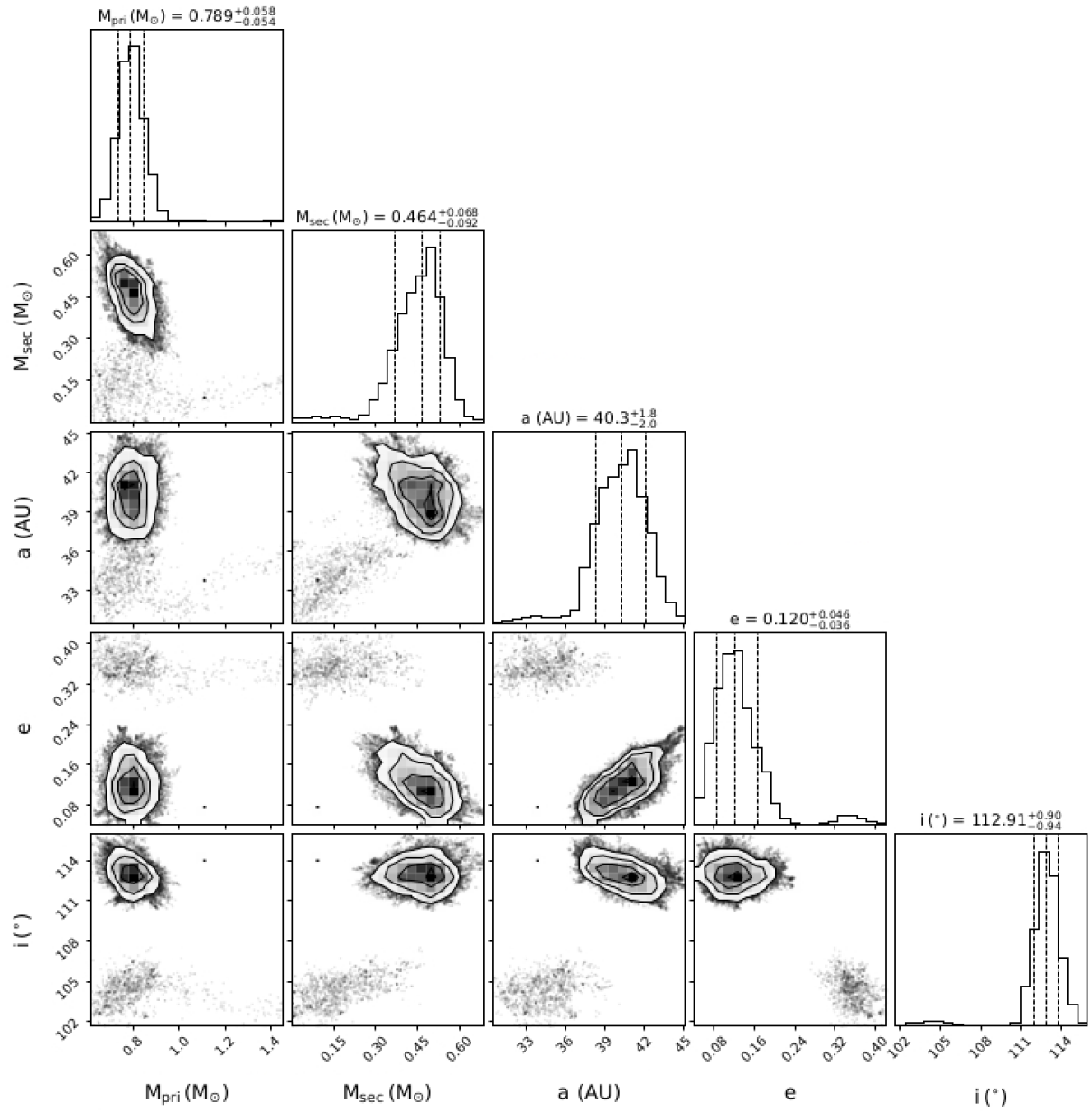

Figure 3.3: correlation plot of the MCMC chains for some of the orbital parameters for Gl 86. The posterior of the MCMC chains, in terms of orbital parameters, are plotted against each other.

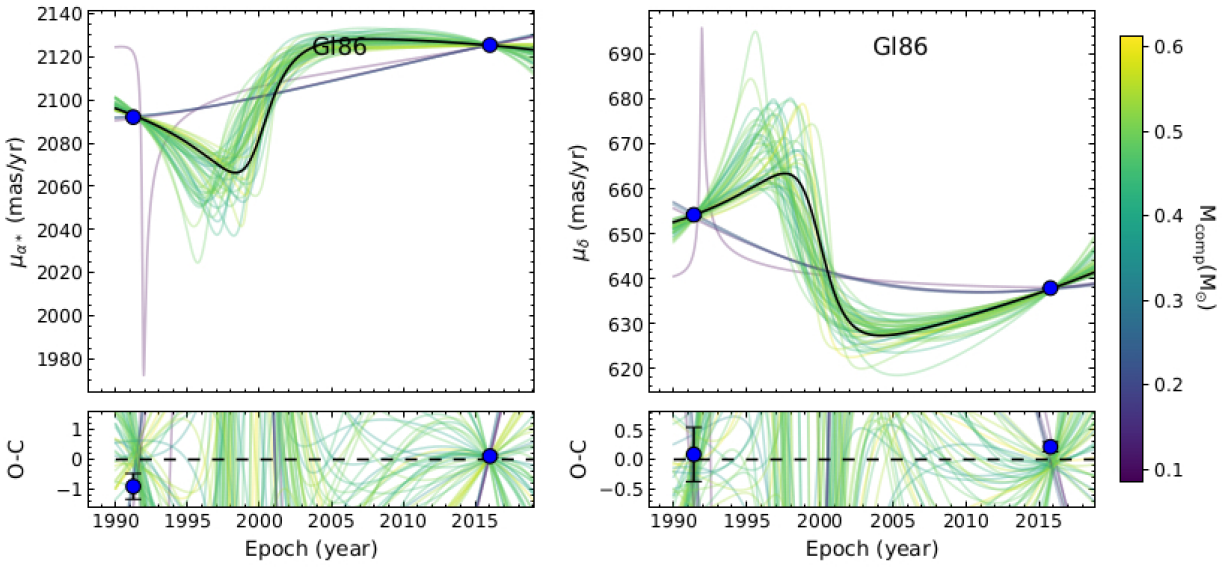

Figure 3.4: These plots are showing the proper motion from HGCA for the primary star (left), and for the companion (right). Both plots include a observed minus calculated plot and also include randomly chosen fitted posterior distributions coloured according to the secondary mass. If the secondary component does not exist in HGCA, the proper motions for the companions are calculated using equation 1.3.

3.3 General results

The general results presented in this subsection are the astrometric orbit plots for all systems and all the posterior parameters for the systems. Table 3.1 shows the posterior parameters from the fits for AF Leporis, Gliese 86, Smethells 119 and Gliese 105. The secondary masses are presented in solar masses for all systems except for AF Leporis since it is an exoplanet and is thus presented in Jupiter masses.

Table 3.1: Table showing the posterior parameters for different stars. Where the secondary mass is given in units of jupiter masses for AF Lep and in solar masses for the binary stars. The parameters are the median of the distribution.

	AF Leporis	**Gl 105 (C)**	**Gl 86**	**Smethells 119**
Jit (m/s)	170^{+38}_{-29}	$2.35^{+0.35}_{-0.26}$	$24.5^{+5.3}_{-4.1}$	$16.7^{+2.2}_{-1.9}$
Mpri ($M_\odot$)	$1.199^{+0.051}_{-0.052}$	$0.87^{+0.19}_{-0.21}$	$0.789^{+0.058}_{-0.054}$	$0.807^{+0.050}_{-0.049}$
Msec	$3.74^{+1.9}_{-0.90}$ M_{jup}	$0.068^{+0.016}_{-0.014}$ $M_\odot$	$0.464^{+0.068}_{-0.092}$ $M_\odot$	$0.1829^{+0.0072}_{-0.0064}$ $M_\odot$
a **(AU)**	$8.0^{+1.1}_{-1.6}$	$12.6^{+4.2}_{-1.6}$	$40.3^{+1.8}_{-2.0}$	$7.33^{+0.17}_{-0.18}$
$\sqrt{e}\sin\omega$	$0.08^{+0.55}_{-0.46}$	$0.590^{+0.038}_{-0.14}$	$-0.234^{+0.086}_{-0.082}$	$-0.281^{+0.046}_{-0.035}$
$\sqrt{e}\cos\omega$	$-0.35^{+0.34}_{-0.25}$	$-0.27^{+0.54}_{-0.10}$	$0.244^{+0.058}_{-0.071}$	$0.308^{+0.035}_{-0.042}$
i **(deg)**	74^{+25}_{-29}	$48.9^{+71}_{-6.6}$	$112.91^{+0.90}_{-0.94}$	$13.6^{+2.8}_{-3.0}$
Asc node (deg)	69^{+20}_{-11}	$318.8^{+8.2}_{-292}$	$68.5^{+2.0}_{-2.0}$	$110.3^{+4.8}_{-6.1}$
mean Ω (deg)	141^{+42}_{-77}	60^{+30}_{-13}	$309.9^{+3.4}_{-3.0}$	$186.4^{+4.3}_{-3.9}$
parallax (mas)	$37.2538^{+0.0019}_{-0.0019}$	$138.331^{+0.061}_{-0.063}$	$92.927^{+0.032}_{-0.032}$	$42.505^{+0.091}_{-0.091}$
period (yrs)	$20.7^{+4.2}_{-6.0}$	$47.3^{+22}_{-7.8}$	228^{+20}_{-18}	$20.00^{+0.37}_{-0.39}$
ω **(deg)**	167^{+74}_{-52}	$114.6^{+7.6}_{-57}$	314^{+16}_{-14}	$317.1^{+6.0}_{-6.8}$
e	$0.34^{+0.40}_{-0.23}$	$0.444^{+0.065}_{-0.14}$	$0.120^{+0.046}_{-0.036}$	$0.178^{+0.024}_{-0.023}$
a **(mas)**	299^{+39}_{-61}	1742^{+582}_{-218}	3747^{+166}_{-184}	$311.7^{+7.1}_{-7.7}$
T0 (JD)	2457007^{+4851}_{-689}	2458061^{+18729}_{-201}	2459775^{+79506}_{-3455}	2457855^{+166}_{-148}
mass ratio	$0.00297^{+0.0014}_{-0.00070}$	$0.083^{+0.020}_{-0.020}$	$0.58^{+0.12}_{-0.13}$	$0.227^{+0.012}_{-0.011}$

In the astrometric orbit plots seen in figure 3.5 you can see that for Gliese 86 and Smethells 119 most of the possible orbits agree with one another but for AF Leporis and Gliese 105 this is not the case. This is due to the astrometric signature of these systems being smaller which is something discussed in more detail in the discussion section. The plot for Smethells 119 has a relative astrometry data point that does not agree with the orbits in the same way that is done for the other systems. One can also observe a group of radial velocity data points in the radial velocity plot for Smethells 119 in figure A.17, left, that are left outside the fits. On the other hand, observing figure A.19 shows a nice fit where both the Hipparcos and Gaia proper motions are in the fit, and lastly the correlation plot in figure A.6 shows that the chains have converged on a good solution. The aforementioned results point to either that some of the RV data and the relative astrometry data point are inaccurate or that the chains got stuck in a local minima.

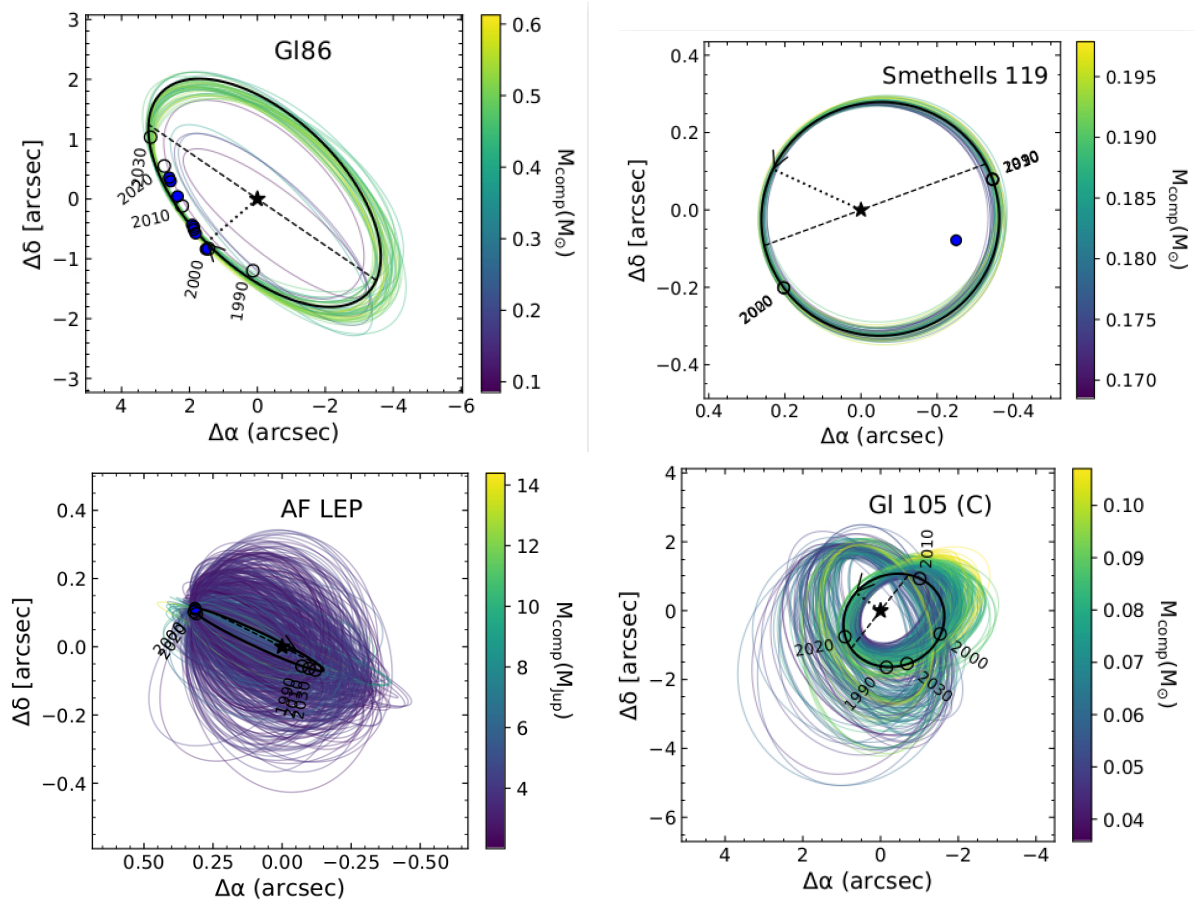

Figure 3.5: Astrometric orbit plots of the secondary stars of Gliese 86, Smethells 119 and Gliese 105 (C) and the super jupiter exoplanet around the star AF Leporis. The plots shows possible orbits, randomly drawn from the posterior distribution. It also includes dashed lines which are the line of nodes joining the ascending and descending nodes. The filled circles are the relative astrometry data points and the unfilled circles are the user specified predicted positions and lastly the dotted lines indicate the tilt of the orbit.

3.4 Diagnostic results

In this subsection, the diagnostic results for when ORVARA was tested to see how it uses the different data are presented. In tables 3.2 and you can observe how the posterior parameters of AF Leporis changes when the individual Hipparcos data files are changed. In table 3.3 you can observe how the posterior parameters of AF Leporis change when the data is modified in the following manner: column one is when the wrong individual Gaia file is used, column two is when ORVARA is run without Radial velocity and without relative astrometry. Columns three and four are the posterior parameters when using only HGCA and not using HGCA (but every other set of data) respectively. Lastly, column five is when the setting `use_epoch_astrometry` is set to false. In these tables it is clear that the results are not affected by changing the individual Hipparcos or Gaia files. It is also clear that relative astrometry, radial velocity and HGCA data sets are the most influential on the results. Table 3.4 shows the posterior parameters for the failed fit on the exoplanet system HD 114082 where it is clear that the results are nonsensical when observing for example the secondary mass of 213 Jupiter masses and the accompanying error bars.

Table 3.2: This table presents how the posterior parameters for AF LEP (HIP 25486) changes when its hipparcos data is changed with the data from another star.

Hip data	**HIP 25486/AF LEP**	**HIP 10138**	**HIP 95319**
Jit (m/s)	170^{+38}_{-29}	169^{+38}_{-32}	169^{+38}_{-30}
Mpri ($M_\odot$)	$1.199^{+0.051}_{-0.052}$	$1.200^{+0.051}_{-0.052}$	$1.200^{+0.050}_{-0.052}$
Msec (jup)	$3.74^{+1.9}_{-0.90}$	$3.9^{+3.7}_{-1.0}$	$3.8^{+2.4}_{-1.0}$
a **(AU)**	$8.0^{+1.1}_{-1.6}$	$8.18^{+0.81}_{-1.3}$	$8.14^{+0.95}_{-1.4}$
$\sqrt{e}\sin\omega$	$0.08^{+0.55}_{-0.46}$	$0.03^{+0.62}_{-0.45}$	$0.05^{+0.57}_{-0.43}$
$\sqrt{e}\cos\omega$	$-0.35^{+0.34}_{-0.25}$	$-0.35^{+0.25}_{-0.20}$	$-0.33^{+0.33}_{-0.24}$
i **(deg)**	74^{+25}_{-29}	79^{+22}_{-28}	76^{+24}_{-28}
asc node (deg)	69^{+20}_{-11}	$68.2^{+8.3}_{-10}$	68^{+11}_{-11}
mean Ω (deg)	141^{+42}_{-77}	151^{+32}_{-60}	149^{+37}_{-63}
parallax (mas)	$37.2538^{+0.0019}_{-0.0019}$	$37.2538^{+0.0019}_{-0.0019}$	$37.2539^{+0.0019}_{-0.0019}$
period (yrs)	$20.7^{+4.2}_{-6.0}$	$21.3^{+3.2}_{-4.7}$	$21.2^{+3.7}_{-5.3}$
ω **(deg)**	167^{+74}_{-52}	174^{+65}_{-58}	172^{+69}_{-57}
e	$0.34^{+0.40}_{-0.23}$	$0.33^{+0.38}_{-0.22}$	$0.32^{+0.36}_{-0.22}$
a **(mas)**	299^{+39}_{-61}	305^{+30}_{-47}	303^{+35}_{-53}
$T0$ **(JD)**	2457007^{+4851}_{-689}	2457256^{+4806}_{-906}	2457115^{+4903}_{-824}
mass ratio	$0.00297^{+0.0014}_{-0.00070}$	$0.00314^{+0.0029}_{-0.00079}$	$0.00302^{+0.0020}_{-0.00079}$

Table 3.3: Table showing the posterior parameters for the system AF LEP when the different kinds of data are removed or changed to data belonging to a new system according to the procedure described in the method section.

	Wrong Gaia	**No RV/relAst**	**Only HGCA**	**No HGCA**	**No epoch astrometry**
Jit (m/s)	169^{+39}_{-30}	$0.41^{+70}_{-0.41}$	$0.48^{+48}_{-0.48}$	157^{+44}_{-31}	169^{+40}_{-29}
Mpri ($M_\odot$)	$1.201^{+0.051}_{-0.050}$	$1.205^{+0.064}_{-0.060}$	$1.195^{+0.061}_{-0.054}$	$1.201^{+0.056}_{-0.056}$	$1.198^{+0.052}_{-0.049}$
Msec (jup)	$4.0^{+4.7}_{-1.0}$	17^{+155}_{-13}	$13.1^{+126}_{-9.2}$	13^{+29}_{-13}	$3.8^{+2.8}_{-1.0}$
a **(AU)**	$8.25^{+0.90}_{-1.2}$	$3.0^{+10}_{-2.7}$	$3.2^{+8.4}_{-3.0}$	$8.9^{+2.6}_{-1.5}$	$8.09^{+0.92}_{-1.3}$
$\sqrt{e}\sin\omega$	$0.13^{+0.58}_{-0.43}$	$0.16^{+0.50}_{-0.54}$	$0.06^{+0.56}_{-0.58}$	$0.16^{+0.35}_{-0.42}$	$0.02^{+0.58}_{-0.43}$
$\sqrt{e}\cos\omega$	$-0.33^{+0.32}_{-0.19}$	$0.22^{+0.49}_{-0.63}$	$0.06^{+0.56}_{-0.64}$	$-0.10^{+0.28}_{-0.33}$	$-0.35^{+0.24}_{-0.23}$
i **(deg)**	79^{+22}_{-32}	84^{+46}_{-43}	98^{+41}_{-51}	61^{+24}_{-33}	76^{+24}_{-24}
asc node (deg)	$69.2^{+14}_{-8.8}$	190^{+90}_{-139}	200^{+90}_{-147}	75^{+84}_{-16}	$68.4^{+7.3}_{-10}$
mean Ω (deg)	151^{+35}_{-69}	190^{+118}_{-142}	193^{+117}_{-139}	141^{+36}_{-95}	147^{+32}_{-58}
parallax (mas)	$37.2539^{+0.0019}_{-0.0019}$	$37.253860^{+0.000079}_{-0.000094}$	$37.253866^{+0.000077}_{-0.00010}$	$37.2539^{+0.0019}_{-0.0019}$	$37.2539^{+0.0019}_{-0.0019}$
period (yrs)	$21.6^{+3.7}_{-4.6}$	$4.7^{+38}_{-4.6}$	$5.2^{+31}_{-5.2}$	$24.0^{+11}_{-5.5}$	$21.0^{+3.6}_{-4.6}$
ω **(deg)**	159^{+85}_{-44}	121^{+187}_{-89}	169^{+132}_{-124}	136^{+101}_{-67}	177^{+65}_{-59}
e	$0.30^{+0.41}_{-0.21}$	$0.52^{+0.33}_{-0.34}$	$0.55^{+0.30}_{-0.36}$	$0.18^{+0.36}_{-0.14}$	$0.32^{+0.33}_{-0.21}$
a **(mas)**	307^{+34}_{-46}	111^{+377}_{-101}	119^{+314}_{-112}	333^{+98}_{-55}	302^{+34}_{-47}
$T0$ **(JD)**	2457338^{+4819}_{-1057}	2455671^{+6410}_{-461}	2455795^{+5306}_{-585}	2461110^{+2366}_{-4659}	2457153^{+4779}_{-861}
mass ratio	$0.00316^{+0.0038}_{-0.00075}$	$0.013^{+0.13}_{-0.010}$	$0.0106^{+0.10}_{-0.0075}$	$0.010^{+0.023}_{-0.010}$	$0.00303^{+0.0023}_{-0.00076}$

Table 3.4: Table presenting the posterior parameters of the failed fit for the system HD 114082. In this case there are two radial velocity jitters for each of the instruments used for gathering radial velocity data. Inst 1 are the measurements from FEROS and inst 2 are the measurements from HARPS.

Jit, Inst #0 (m/s)	328^{+67}_{-101}
Jit, Inst #1 (m/s)	212^{+56}_{-44}
Mpri ($M_\odot$)	$1.476^{+0.071}_{-0.078}$
Msec (jup)	213^{+5801}_{-207}
a **(AU)**	32^{+437}_{-28}
$\sqrt{e}\sin(\omega)$	$-0.40^{+0.67}_{-0.41}$
$\sqrt{e}\cos(\omega)$	$-0.15^{+0.57}_{-0.41}$
i **(deg)**	89^{+13}_{-13}
asc node (deg)	168^{+111}_{-105}
mean Ω (deg)	149^{+99}_{-61}
parallax (mas)	$10.520044^{+0.000040}_{-0.00022}$
period (yrs)	120^{+1505}_{-112}
ω **(deg)**	237^{+57}_{-124}
e	$0.59^{+0.28}_{-0.41}$
a **(mas)**	341^{+4600}_{-292}
$T0$ **(JD)**	$2464350^{+269818}_{-8230}$
mass ratio	$0.14^{+3.8}_{-0.13}$

Chapter 4

Discussion and conclusions

4.1 Discussion

This section is split into three parts: In the posterior parameters part I discuss how accurate the posterior parameters of the different systems are when compared to other sources. In the plots part I discuss the plots and what information they provide. And lastly, in the data sets part I discuss how the different data sets are used and potential problems about them.

4.1.1 Posterior parameters

According to Franson et al. (2023), the mass of AF Lep b should lie around 4-6 M_{jup} according to the hot-start evolutionary models, and if the planet was formed at the same time as the star. The results for AF Lep b in table 3.1 are on the lower end of that span but considering the upper uncertainty bound, the span is within the uncertainty of the fitted secondary mass. Franson et al. (2023) reasons that this discrepancy in fitted mass versus the model mass could be because the star is slightly younger than expected, delayed formation in a disk, systematic uncertainties in the evolutionary models or there is another companion in the system. The other parameters for the AF lep system in table 3.1 also agree with the results from Franson et al. (2023). The results of this thesis also agree with the results presented in Mesa et al. (2023). Something that needs to be considered is that in both of these articles Orvara was used to calculate the posterior parameters of this system. This means that the results will be similar but with different levels of precision depending on how many resources are allocated to Orvara.

When it comes to the Gl 105 A-C system, there are not many articles about the parameters of this system. However, Feng et al. (2021) has presented a fit and comparing the results in table 3.1 to table 3 in that article shows a varying degree of agreement between the different parameters. For example, the secondary masses are very similar but the period and eccentricity are not similar at all. According Feng et al. (2021), the period is 76.1 years while in table 3.1 it is 47.3 years and the eccentricity is 0.64 versus 0.44 in

this thesis. In the aforementioned article, they use the HGCA data set as well as radial velocity data and they fit the parameters using MCMC. Their methods are thus similar to Orvara and as such the most likely reasons for this difference in parameters could be that they had more or less data, more or less accurate data, or a better or worse numerical implementation. Due to the lack of articles that presents parameters for Gl 105 A-C it is difficult to know if the results from their article were more accurate than the ones presented here. It is however worth mentioning that if the error spans of the results of this thesis are considered, they encompass the results from Feng et al. (2021). The calculations in this thesis for this system rendered some unusually large uncertainties for some of the parameters. The period is one of them and has an upper uncertainty limit of 47.3+22.0 and in Feng et al. (2021), the errors are $\sim \pm 10\%$ on all parameters.

When it comes to Gliese 86 B, I compare the results in table 3.1 to Zeng et al. (2022) and Quarles et al. (2020). In Zeng et al. (2022), they used Orvara and the same relative astrometry data as me. However, in this thesis I decided to use radial velocity data from another source compared to what this article used. The change in radial velocity data was done in order to not do exactly the same thing as Zeng et al. (2022). This means that in large the results are similar but there are quite a few discrepancies. The secondary mass in table 3.1 was 0.464 $M_{\odot}$, in Quarles et al. (2020) it was 0.490 $M_{\odot}$ and in Zeng et al. (2022) it was 0.543 $M_{\odot}$. When it comes to the semi-major axis, there were a lot larger discrepancies. in table 3.1: $a = 40.3$ A.U, in Quarles et al. (2020): $a = 21$ A.U and in Zeng et al. (2022): $a = 23.7$ A.U. The eccentricity in Zeng et al. (2022) is 0.429 and in table 3.1 it is 0.120. Lastly, the Orbital period: There seems to be no real consensus of how long the orbital period is. In Zeng et al. (2022) it is stated that the period is about 100 years long and in the article Queloz et al. (2000) they state that Gl 86 B could have an orbital period longer than 100 years. From the calculations in this project, the orbital period seems to be about 228 years. Due to the fact that Zeng et al. (2022) uses more radial velocity data points and allow their MCMC chains run for longer to not get stuck in local minima, their results should be more accurate. However, when I attempt to replicate their results using the same data and settings as described in Zeng et al. (2022), the results generated are much closer to what is presented in this thesis than in that article. This discrepancy is most likely due to that when they are plotting the RV signature for the binary, they have subtracted the signal from the planet in that system which I did not have time to do here. This becomes evident when comparing table 2 to the RV plots in figure 4 in Zeng et al. (2022) where in the table, there are multiple data points above 1000 m/s and in the plot, no points break 500 m/s. Most likely, this means that they have done some calculations on their radial velocity data which I was unable to interpret correctly. In Zeng et al. (2022), they state that they use two sets of radial velocity data from Diego et al. (1990) and Butler et al. (2006), the combination of which are presented in the aforementioned table 2. When I used this data for calculations, figure A.10 shows the radial velocity data points with fitted errors from the best fit. If figure A.10 is compared to the RV plots in figure 4 in Zeng et al. (2022), one can clearly see how different the radial velocity they present is compared to what they use for their fits. Due to

these presented concerns with the radial velocity, it is difficult to say whether the results presented in table 3.1 are more or less accurate than the ones presented in Zeng et al. (2022). It is also important to keep in mind that it is difficult to create a good fit for a system with this long of a period since the baseline for the measurements is only ∼30 years.

For the final system, Smethells 119, I compare the results to Biller et al. (2022). In this article, the authors present results for four different combinations of data. They state that the best combination is direct imaging + radial velocity + Hipparcos data. They do not provide their reasoning for why this combination of data is better than to also include Gaia data which at least would not harm the accuracy of the calculations. As such, I will compare to the DI+RV+Hipparcos+Gaia results since they are the most comparable to the results in table 3.1. The primary and secondary masses in the results of this thesis are 0.807 $M_\odot$ and 0.183 $M_\odot$ respectively, in Biller et al. (2022) the primary and secondary masses are 0.809 $M_\odot$ and 0.125 $M_\odot$. These results are very similar, but when it comes to the period and eccentricity, the results are no longer as similar. In the article: $e = 0.740$ and $P = 38.4$ years, and in table 3.1: $e = 0.178$ and $P = 20.0$ years. For this system, I can not say if the results from this thesis are more trustworthy than those of Biller et al. (2022) since they use a different approach than me. What I can say is that their method is similar to that of Orvara and the MCMC settings that they used are similar to the settings I used and as such, it is difficult to say which results are better. When observing the errors of the results, the uncertainty ranges of the period are $38.4^{+1.81}_{-1.75}$ and $20.0^{+0.37}_{-0.39}$ years in Biller et al. (2022) and this thesis respectively. For the eccentricity, the uncertainties are $0.740^{+0.008}_{-0.009}$ and $0.178^{+0.024}_{-0.023}$ respectively. Neither of these results are within each others uncertainty and the uncertainties are similar to each other which is expected since a similar approach was used in generating these results.

After comparing the posterior parameters of this thesis to other articles I can say that AF Lep and Gl 105 (C) had results that agreed more to the literature compared to Gl 86 and Smethells 119 in which only some results agreed with the literature. The main reason why the results from this thesis might differ from the ones in other articles are stochastic errors in the MCMC where the chains get stuck in a local minimum which could have happened either for this thesis or in the articles.

When it comes to the system HD 114082, there are a couple of reasons as to why the fit failed. One might be quick and say that it is due to the lack of relative astrometry data. However, when comparing the results for HD 114082 to those without relative astrometry in table 3.3, you can see that this is not enough of an explanation. By observing the plots of HD 114082 in appendix A.4, one can see that the chains had trouble finding any solution for the orbit. In Zakhozhay et al. (2022) they manage to get a good fit using the same radial velocity data as in this thesis, and with Gaia/Hipparcos data. This means that Orvara was unable to achieve a fit for a system which was fitted accurately in Zakhozhay et al. (2022) even though the same data was used.

4.1.2 Plots

When it comes to the plots, all possible plots were produced but the astrometric prediction plot was not included in the thesis. This decision was made because it does not add any information that the astrometric orbit plots have already given. All the astrometric prediction plot is a snapshot of how the mass is distributed in the system at a certain time. Since the astrometric orbit can include many different predicted positions, it makes the astrometric prediction redundant.

When observing the correlation plots, figures 3.3 and A.6-A.8, it is possible to see how well the different MCMC chains have converged. The more concentrated the regions are, as in figure A.6, the more the chains have converged. The correlation plots also allow one to see how the posterior of the MCMC chains are distributed against each other and again, the more uniform the regions are, the more accurate solution the chain has been able to find. In the correlation plots for Gl 86 and Smethells 119, one can see that the chains have found answers that are more accurate than the ones for Gl 105 (C) and AF Lep. This is because of the astrometric signature of these systems which will be discussed further below. The chains could have converged even less, I have included a correlation plot for a system where the fit completely failed, figure A.9, and as can be observed in that plot, there are no regions, none of the chains are converging. Compare this correlation plot to the correlation plot of the other systems and you will see that the fits could have been a lot worse.

The diagnostic plots on the other hand are much more straight forward. They can be seen in figures A.1-A.4. They show the individual chains plotted against the sample. In the ideal scenario, all chains clearly converge. However, none of the diagnostic plots clearly shows this behaviour. The plot for Gl 86 A.1 shows some convergence for all the chains and the plot for Smethells 119 A.3 also shows some nice convergence from the chains. When it again comes to the systems of smaller astrometric signature, which will be discussed later, the diagnostic plots for both AF Lep and Gl 105 (C) show less converging chains. This also agrees with what can be seen in the correlation plots.

When observing figure 3.5, one can see that the figures plotting the potential orbits of binary stars are much more similar than the potential orbits of the planet. This is due to the fact that since the mass of a planet is much smaller than that of a star. This effect can be shown with the astrometric signature of the different systems. Using equation 1.2, we can calculate that Gl 86 has an astrometric signature of $\alpha = 1387.6$ mas, Smethells 119 has $\alpha = 57.592$ mas, AF Lep has $\alpha = 0.88762$ mas and GL 105 (C) has $\alpha = 126.29$ mas. This means that the smaller the mass of the planet/star is, the less it will affect the movement of the star. This in turn means that the different potential fitted orbits will more or less agree with each other depending on the mass of the secondary.

In the astrometric plot of Gl 105 C, you can see that there are two distinct orbital

distributions. As described in the method section, only relative astrometry data for the Gl 105 A-C system is provided and as such, the less probable, second distribution of potential orbits is probably due to Gl 105 B which is a more massive star compared to the red dwarf Gl 105 C. This means that it is inevitable that the results for this star will be faulty to some degree. The astrometric signature of this system is higher than that of the Smethells 119 binary which should mean that the possible orbits should be closer packed in the Gl 105 A-C system than in the Smethells 119 system. This is however not the case since, as mentioned above, there is a larger star creating larger perturbations for the main star compared to what the red dwarf creates. This means that even though the astrometric signature is quite large the different possible orbits will be quite varied.

While using the plot_obit command, it is not uncommon for the resulting plots to be missing crucial parts. Seemingly at random, the color bar on the side can be missing, the data points can be missing, the epoch years can be written as $0.8 \cdot 2.022\text{e}3$ etc. This can be tedious and one can only run the figure through an image editing software to try to restore the figures. In the appendix, one can see these effects in some of the figures for the systems.

4.1.3 Data

In this thesis, how the different kinds of data was weighed against one another was investigated. The radial velocity, relative astrometry and the HGCA data are very important and have a large impact on the results. On the other hand, individual Hipparcos and Gaia data files seem to not contribute to the final results much at all. When this data is left out of the calculations, the results are less accurate when compared to the posterior parameters in the general runs. Compare table 3.3 to the posterior parameters of AF Lep in table 3.1. When given all types of data that are possible to give, Orvara produces results which agree with the literature. However, there are many criteria which need to be fulfilled in order to reach this level of accuracy. First of all, the star needs to be in both Hipparcos and Gaia, i.e. it cannot be too dim such that Hipparcos can measure it and not too bright so that Gaia cannot measure it. It needs to have both radial velocity data and relative astrometry data available and lastly, it also needs to exist in the HGCA file. As has been stated before, the program can produce results without all these forms of data but these results are of varying degrees of accuracy. All in all this means that, to get the best results Orvara can produce, there are not that many stars which can fulfill all the requirements meaning that the program can only produce accurate results for a handful of the measured systems.

A quite big restriction with the relative astrometry data is that the position angle and angular separation are gathered through direct imaging of the stellar system of interest. This means that, with the limitations of current telescopes, you can not use relative astrometry data on systems with smaller planets and short semi-major axes. This will also impede the accuracy of results for systems like these since relative astrometry is quite

highly weighed as can be seen in table 3.3.

From the investigation of how ORVARA prioritizes data, you can observe that the individual Hipparcos and Gaia files only have a small weight in the calculations. On the other hand, the radial velocity data, relative astrometry data and the HGCA data set are weighted very highly in the calculations. Since the radial velocity data is very important to get good results, ORVARA is, in a practical sense, simply a radial velocity fitting program. There are however use cases for this program. If one is able to find or generate both radial velocity data and relative astrometry data and if the star exists in both Gaia and Hipparcos, it can be used to get highly accurate parameters for any type of system where the orbiting body/bodies have an effect on the movement of the host star. If all these criteria are met, astronomers can use this program to calculate attributes or improve the already known attributes of an exoplanet. A good example of the strength of ORVARA can be seen in the results of the aforementioned system Gl 105 (A-C). This system has two much larger stars and a small red dwarf. The larger component of the trinary system will affect the movements of the primary star much more than the red dwarf. Despite this, ORVARA is able to calculate clear parameters for the long period orbit of the red dwarf in about 10 minutes when this would have taken longer with other programs according to figure 1 in Brandt et al. (2021). By comparing the proper motion plots to the other plots, one can clearly see that all the fits, for all systems, go through the error bars of the Gaia data in the HGCA data set. This seems to suggest that the individual highest weight out of all data is the Gaia data in the HGCA data. This supports the theory that Hipparcos only creates a larger baseline and has an otherwise low weight for the result.

When it comes to the HGCA data set which plays a large role in ORVARA'S calculations, the creators claim that the methods used to combine Gaia and Hipparcos data produce an accurate combined data set. This is however unlikely since the Hipparcos data has a 100 times higher uncertainty than Gaia which would mean that propagating the Gaia data backwards to Hipparcos will yield the same uncertainty as Hipparcos. This is further emphasised by equation 4 in Michalik et al. (2014) which states that the combined proper motion error of the two sets are the root sum square of the position errors divided by the difference in epoch. As an example, we can calculate an approximated error for the combined Gaia Hipparcos proper motion:

$$\sigma = \frac{\sqrt{\sigma_{pos1}^2 + \sigma_{pos2}^2}}{\Delta t} = \frac{\sqrt{1000^2 + 20^2}\mu\text{as}}{30\text{yr}} = 33.34\mu\text{as/yr}$$

Two things can be seen in this example: that the uncertainty is worse than only using Gaia and that the Δt helps a lot in reducing the uncertainty. In essence, if you combine precise data with less precise data, you will get an error that is trending toward the error of the less accurate data. The equation is however only a rough way to evaluate if it is meaningful to combine two data sets. As such, it is not a definite solution to the error which should be lower than that of the Gaia proper motion errors to make the combination

add anything meaningful. In reality, one would reduce the weight of the Hipparcos data in order to keep the proper motion errors roughly, and lower than, those of Gaia. On the other hand, systematic errors would still be assumed to be of the same order of magnitude which would mean that one might amplify any unknown systematic errors by combining the data. Thus the formula given above should only be used to give an idea if it would give us anything meaningful to combine two data sets.

The investigation of how Orvara works and how it prioritizes the data was difficult to assess. This requires further investigation which could be done by either simulating a range of different star systems and then generating your own Gaia, Hipparcos, RV and relative astrometry data to see how accurate Orvara is. To see how Orvara uses and weigh data against each other, you could dig into the code and for example substantially increase the errors of the Hipparcos or Gaia data which would mean that Orvara ignores that data. You could also just completely modify the code such that some of the data is not used at all and then by observing how the results change, one could conclude how the different data is weighed against each other. If you combine these two methods, you will be able to know exactly how accurate to the simulated Keplerian parameters Orvara is able to predict which means that the analysis of when different data is left out can be done much more accurately.

4.2 Conclusions

In this thesis I have investigated how Orvara behaves when given different kinds of data and I have also used Orvara to produce fits for the orbital parameters of 5 systems. The required data was collected from various sources to then be used with Orvara to achieve the results. The testing of Orvara was done on the system AF Leporis during which the posterior parameters were observed to see how they react when data is removed or altered.

When given accurate data of all the different kinds that Orvara requires it produces good results that are reasonable and to some degree agree with other articles. In the program's accompanying article, Brandt et al. (2021), they emphasise that Orvara can produce good results using any combination of data. However, to find or create the radial velocity and relative astrometry data sets, can take a lot of effort and time. This also means that when using Orvara, it appears as if it is a quick and accurate radial velocity fitting program. When it comes to how the different sets of data are used, the results seem to point towards that neither the individual Gaia nor the two reductions of Hipparcos data have any significant weight towards the results. On the other hand, the HGCA, radial velocity and relative astrometry data sets seem to be weighed heavily in the results. When the entire Gaia data is released, Hipparcos should not be used in the calculations in order to avoid systematic errors. The only thing Hipparcos would contribute with is a longer baseline but this is not enough to make up for the loss in accuracy it entails. As can be

seen in the discussion section, some results do not agree with the literature even though ORVARA was given all types of required data. This could be because ORVARA might have been given faulty data or too little data. This must therefore be investigated further to see whether the results of this thesis are more accurate than the parameters in the articles that were compared to.

When it comes to the results that were generated, the following was able to be confirmed: In Gliese 105, it was shown that there exists a companion of red dwarf-star mass. In the AF Leporis system, a super Jupiter sized planet was confirmed to exist. For the systems Gliese 86 and Smethells 119, in both a companion of star mass were confirmed to exist. For the investigated systems, there was no abundance of articles outlining their companions orbital parameters. The orbital parameters for the AF Leporis system agreed the most with articles, but this was expected since those articles also used ORVARA to generate their results. The results from this thesis for the Gliese 105 (A-C) system mostly agrees with the single article that was found. For the two binary systems, Smethells 119 and Gliese 86, their results did not agree very well with their corresponding articles although the integrity of the results from those articles can be discussed whether those results are more or less accurate than the results presented here.

To reiterate, for the sake of clarity, AF Leporis was confirmed to have an exoplanet, Gliese 105 was confirmed to have a third component, Smethells 119 and Gliese 86 were confirmed to be binary star systems. ORVARA works well and produces accurate results when given Radial velocity data, Relative astrometry data and HGCA data. Without any of these, the accuracy of the results suffer.

Acknowledgements

I would like to acknowledge the following people: Dr. David Hobbs for being a great supervisor, Dr. Timothy D. Brandt for creating Orvara and all its accompanying programs which made this project possible, Johan Holmberg and Elliot Winsnes and Eric Svensson and Filip Gustavsson for assisting me through my years in physics. Honorable mentions: Oskar Nilsson, Benjamin Dahlén, Matilda Skantz and Claudia Skoglund for providing me with great entertainment and friendship through the years.

Bibliography

Altena, W. F. V. & Horch, E. 2013, Astrometry for astrophysics: Methods, Models, and Applications, 1st edn. (Cambridge: Cambridge University Press)

Biller, B. A., Grandjean, A., Messina, S., et al. 2022, A&A, 658, A145

Bonavita, M., Gratton, R., Desidera, S., et al. 2022, Astronomy & amp Astrophysics, 663, A144

Brandt, G. M., Michalik, D., Brandt, T. D., et al. 2021, The Astronomical Journal, 162, 230

Brandt, T. D. 2021, The Astrophysical Journal Supplement Series, 254, 42

Brandt, T. D., Dupuy, T. J., & Bowler, B. P. 2019, AJ, 158, 140

Brandt, T. D., Dupuy, T. J., Li, Y., et al. 2021, AJ, 162, 186

Butler, R. P., Vogt, S. S., Laughlin, G., et al. 2017, The Astronomical Journal, 153, 208

Butler, R. P., Wright, J. T., Marcy, G. W., et al. 2006, ApJ, 646, 505

Devore, J. L. 2000, Probability and statistics for engineering and the sciences, 5th edn. (Boston: Thomson Learning/Cengage Group)

Diego, F., Charalambous, A., Fish, A. C., & Walker, D. D. 1990, in Society of Photo-Optical Instrumentation Engineers (SPIE) Conference Series, Vol. 1235, Instrumentation in Astronomy VII, ed. D. L. Crawford, 562–576

Feng, F., Butler, R. P., Jones, H. R. A., et al. 2021, MNRAS, 507, 2856

Figueira, P., Pepe, F., Melo, C. H. F., et al. 2010, Astronomy and Astrophysics, 511, A55

Foreman-Mackey, D., Hogg, D. W., Lang, D., & Goodman, J. 2013, , 125, 306

Franson, K., Bowler, B. P., Zhou, Y., et al. 2023, arXiv e-prints, arXiv:2302.05420

Golimowski, D. A., Henry, T. J., Krist, J. E., et al. 2000, The Astronomical Journal, 120, 2082

Hirsch, L. A., Ciardi, D. R., Howard, A. W., et al. 2019, ApJ, 878, 50

Mesa, D., Gratton, R., Kervella, P., et al. 2023, Astronomy &amp Astrophysics, 672, A93

Michalik, D., Lindegren, L., Hobbs, D., & Lammers, U. 2014, Astronomy &amp Astrophysics, 571, A85

Perryman, M. 2018, The Exoplanet Handbook, 2nd edn. (Cambridge: Cambridge University Press)

Quarles, B., Li, G., Kostov, V., & Haghighipour, N. 2020, AJ, 159, 80

Queloz, D., Mayor, M., Weber, L., et al. 2000, A&A, 354, 99

Samus, N. N., Kazarovets, E. V., Durlevich, O. V., Kireeva, N. N., & Pastukhova, E. N. 2009, VizieR Online Data Catalog, B/gcvs

Vousden, W. D., Farr, W. M., & Mandel, I. 2016, MNRAS, 455, 1919

Walsh, B. 2004, Markov chain Monte Carlo and Gibbs sampling, Penn state university

Zakhozhay, O. V., Launhardt, R., Trifonov, T., et al. 2022, A&A, 667, L14

Zakhozhay, O. V., Launhardt, R., Trifonov, T., et al. 2022, Astronomy &amp Astrophysics, 667, L14

Zeng, Y., Brandt, T. D., Li, G., et al. 2022, The Astronomical Journal, 164, 188

Appendix A

Figures

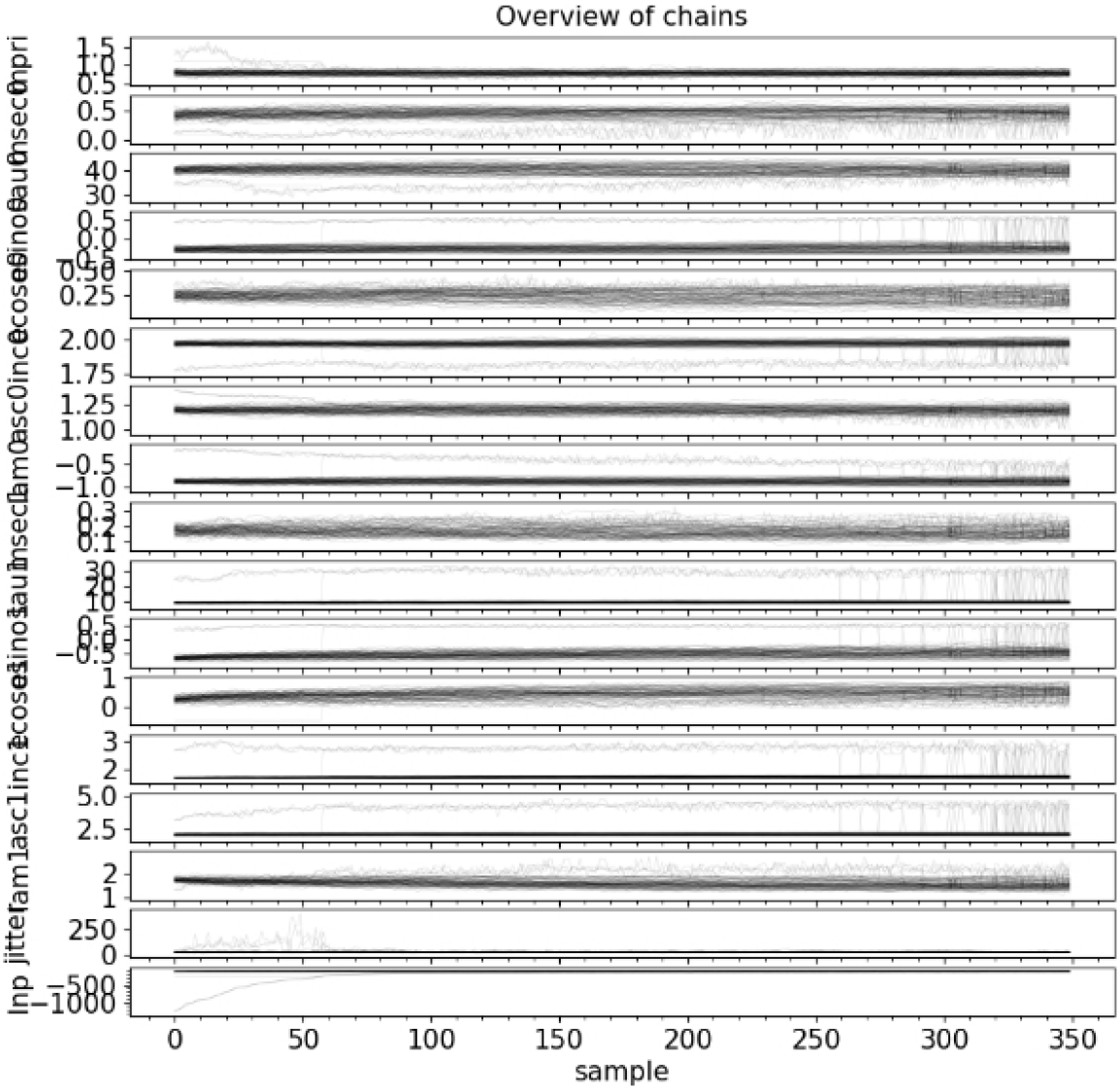

Figure A.1: Diagnostic plot showing an overview of the MCMC chains for Gl 86

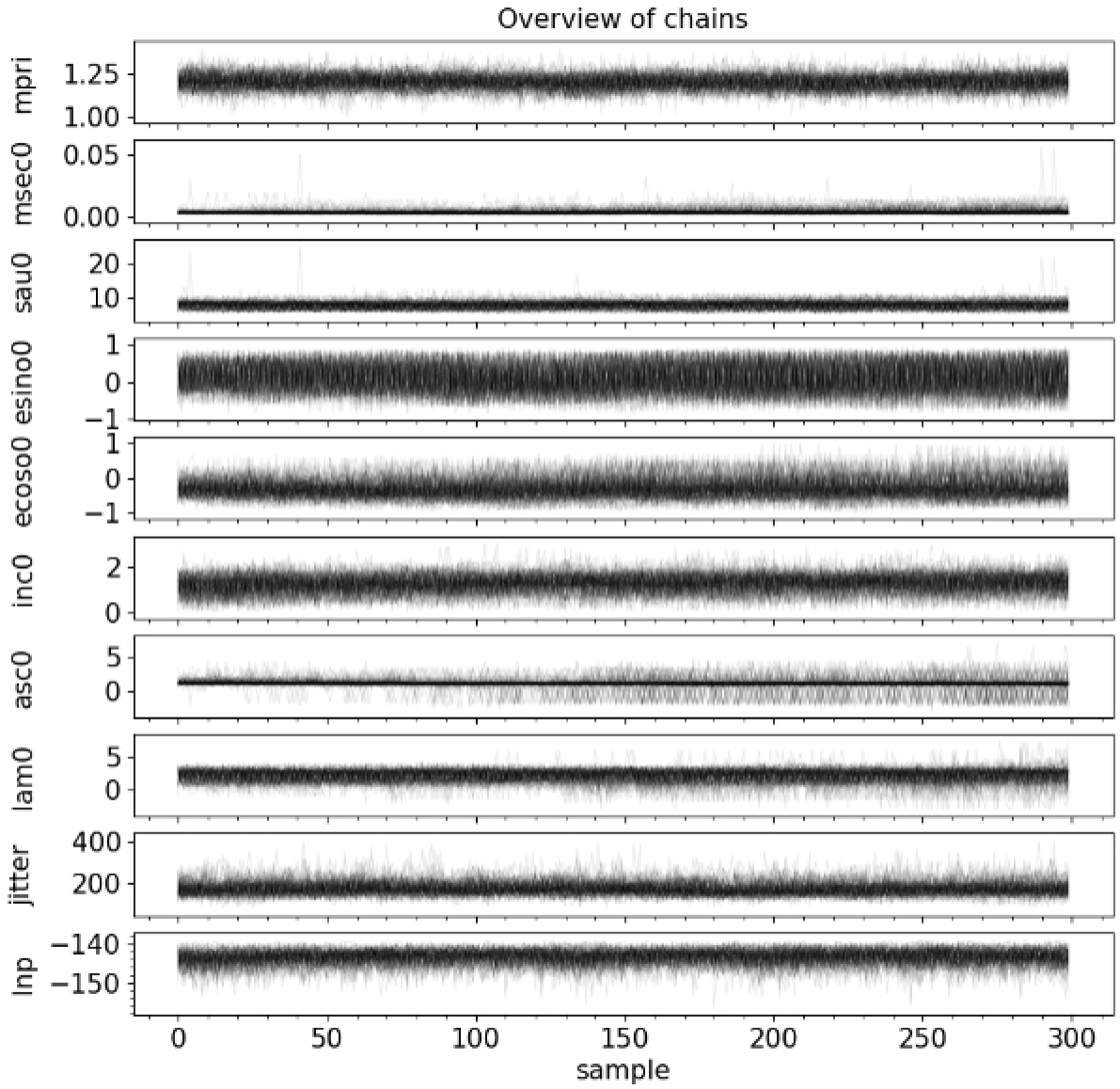

Figure A.2: Diagnostic plot showing an overview of the MCMC chains for AF Lep

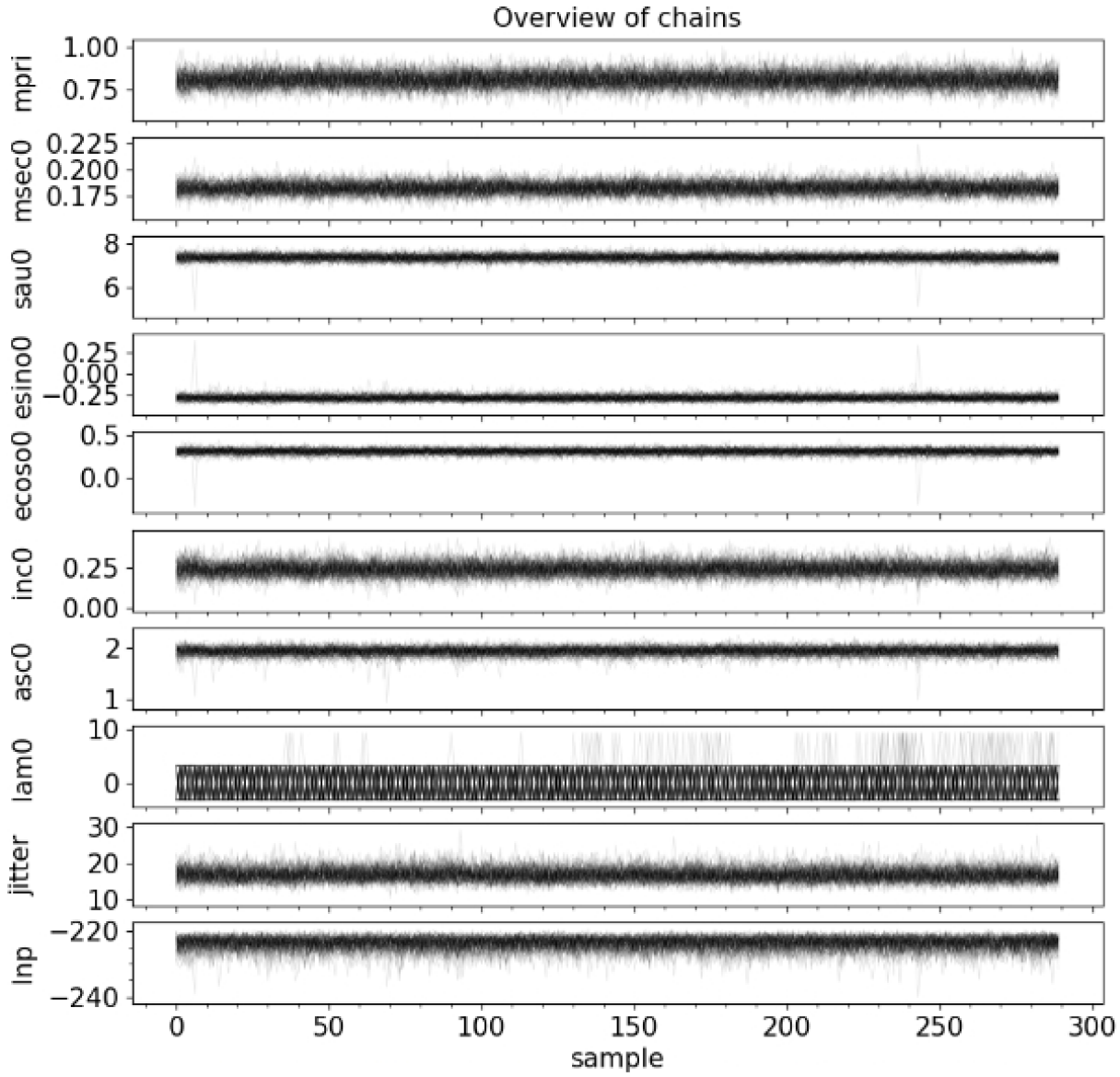

Figure A.3: Diagnostic plot showing an overview of the MCMC chains for Smethells 119

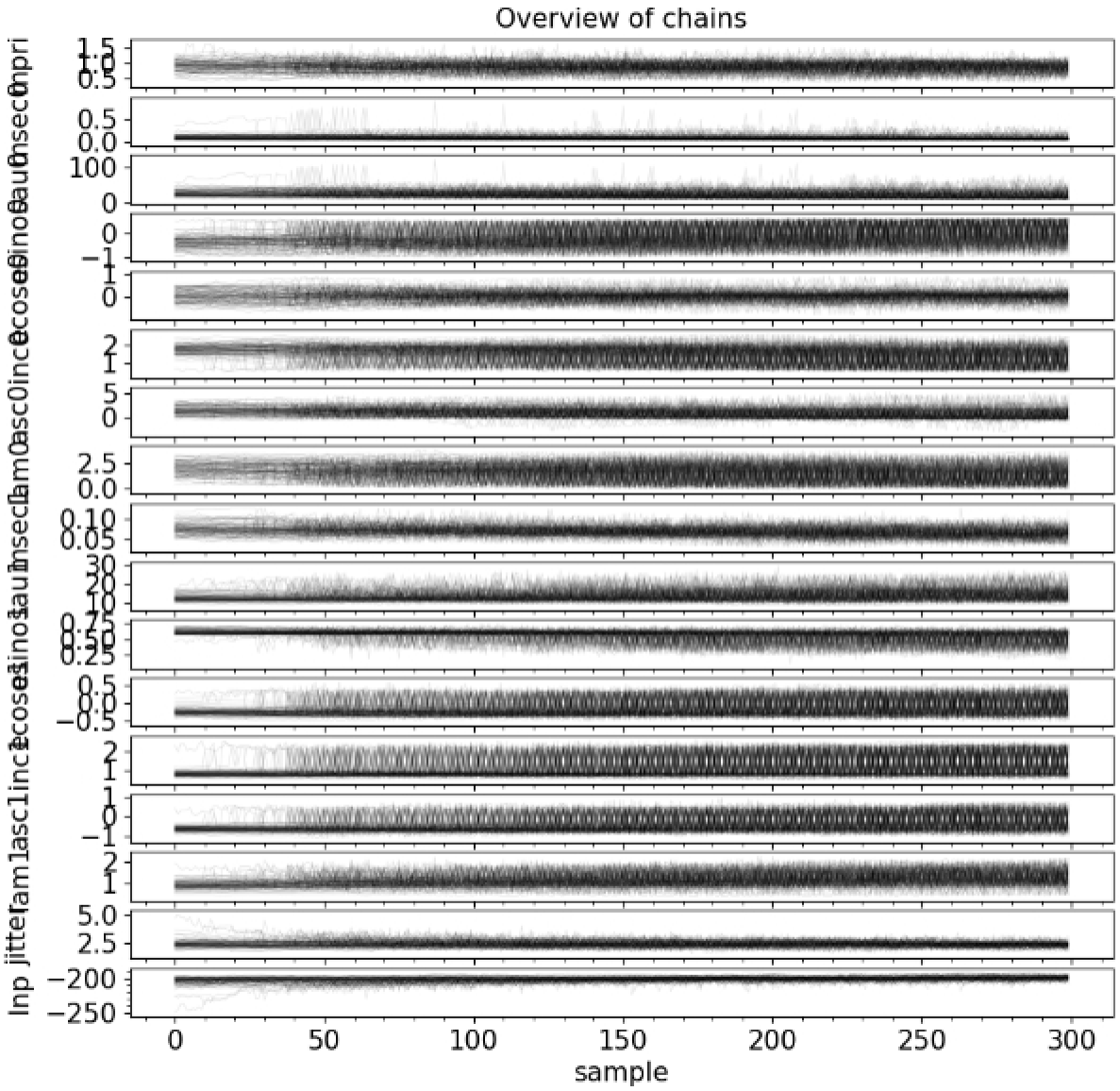

Figure A.4: Diagnostic plot showing an overview of the MCMC chains for Gl 105

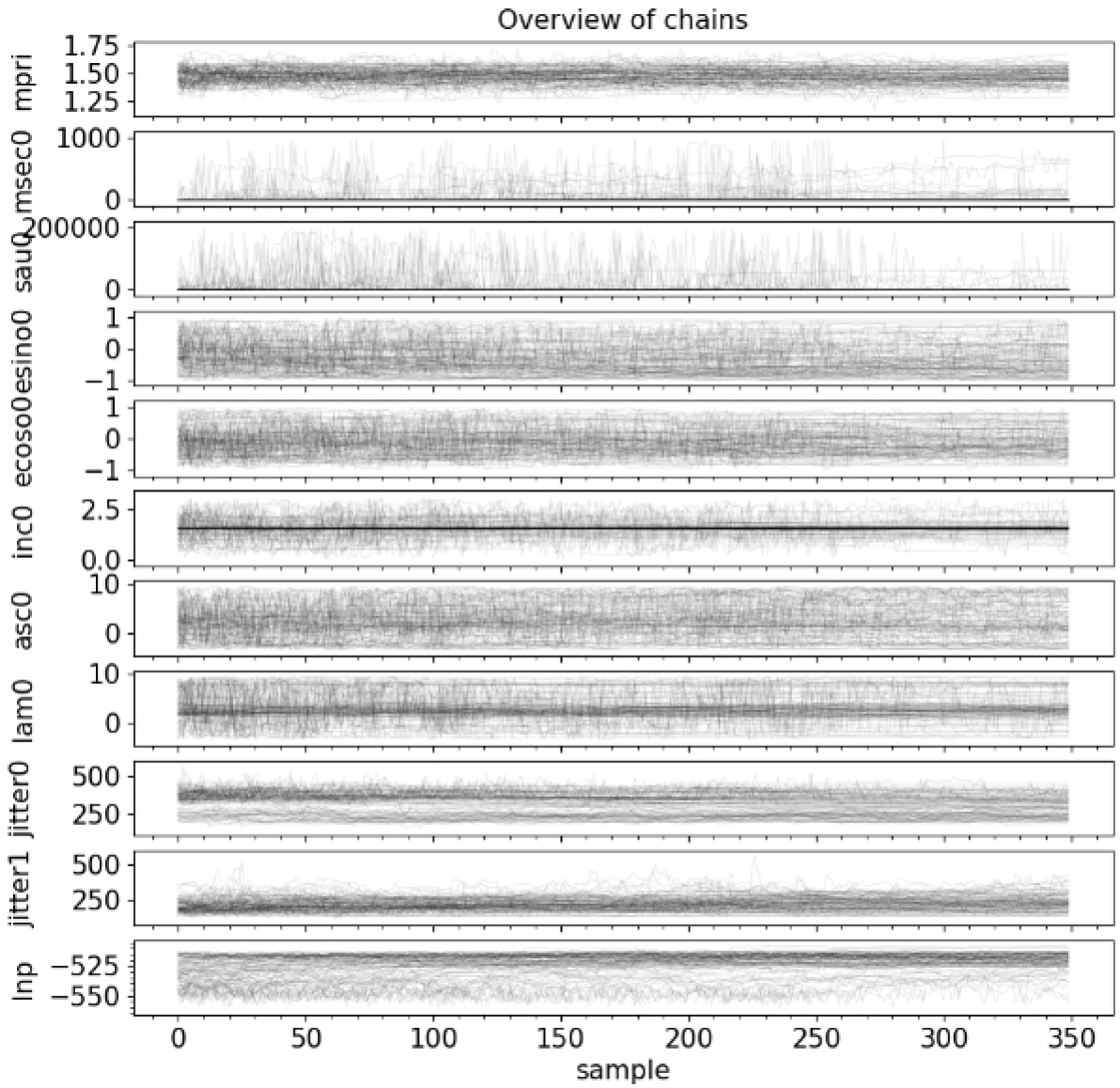

Figure A.5: Diagnostic plot showing an overview of the MCMC chains for HD 114082

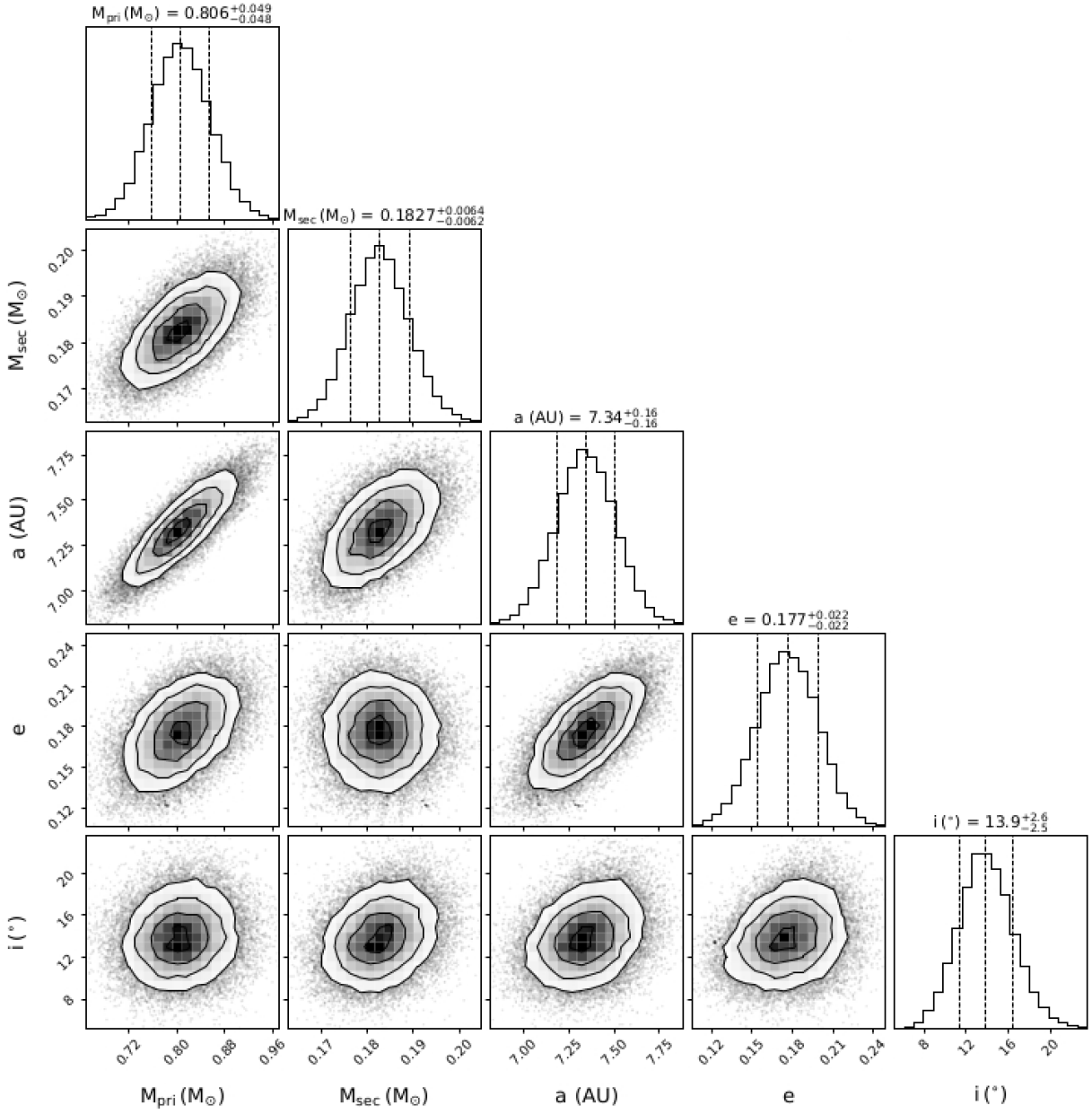

Figure A.6: correlation plot for Smethells 119

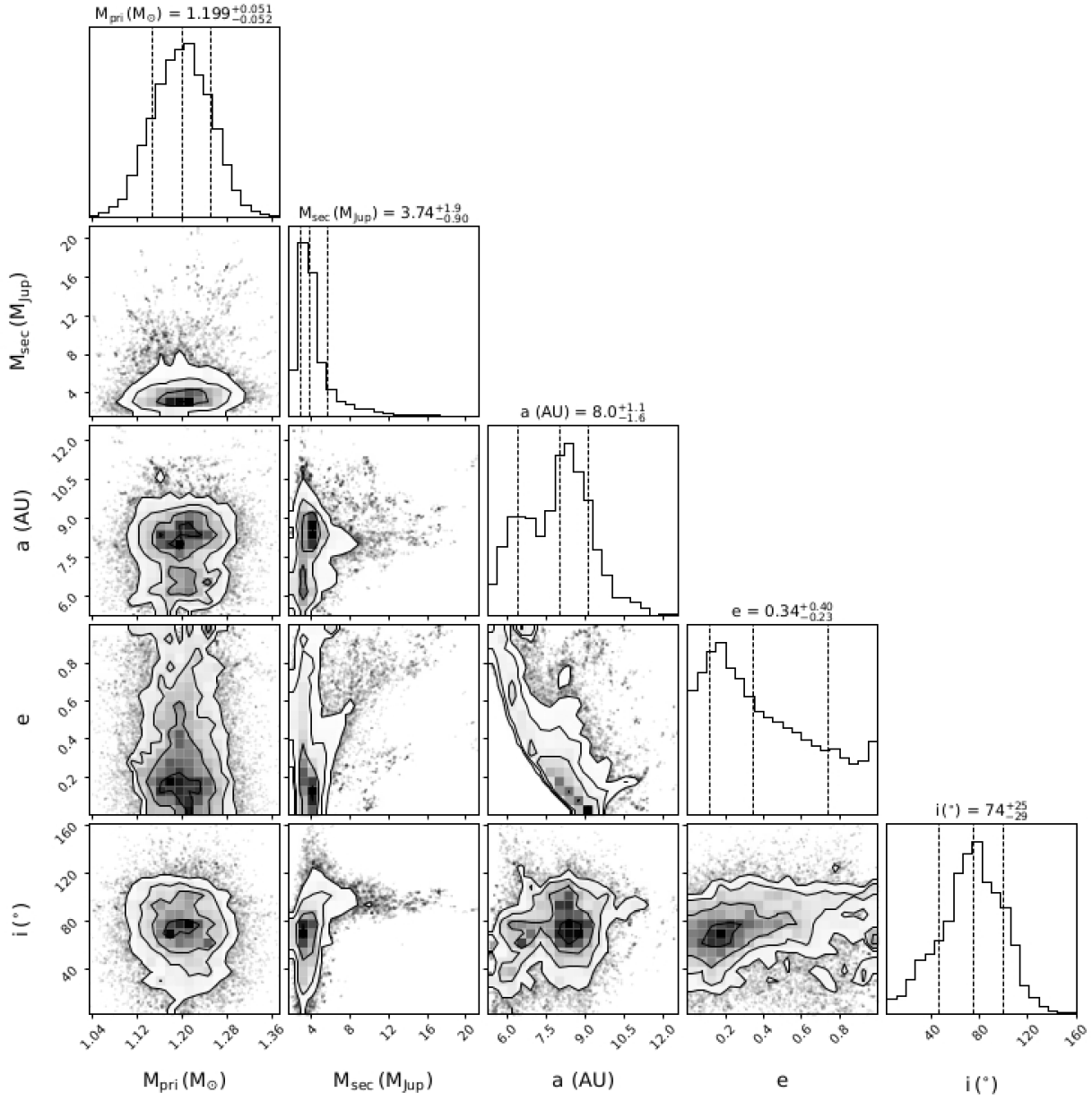

Figure A.7: correlation plot for AF Lep

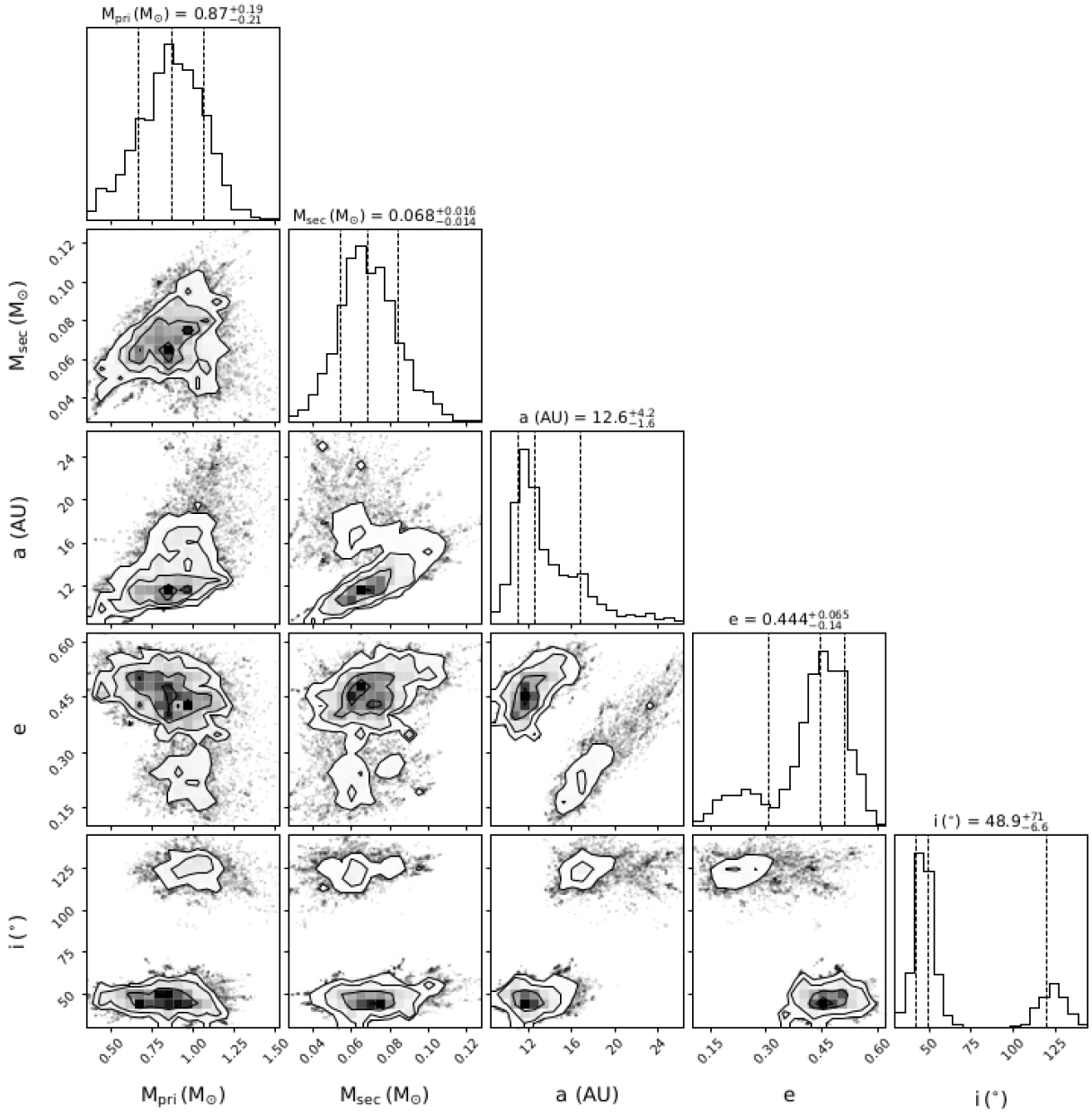

Figure A.8: correlation plot for Gl 105

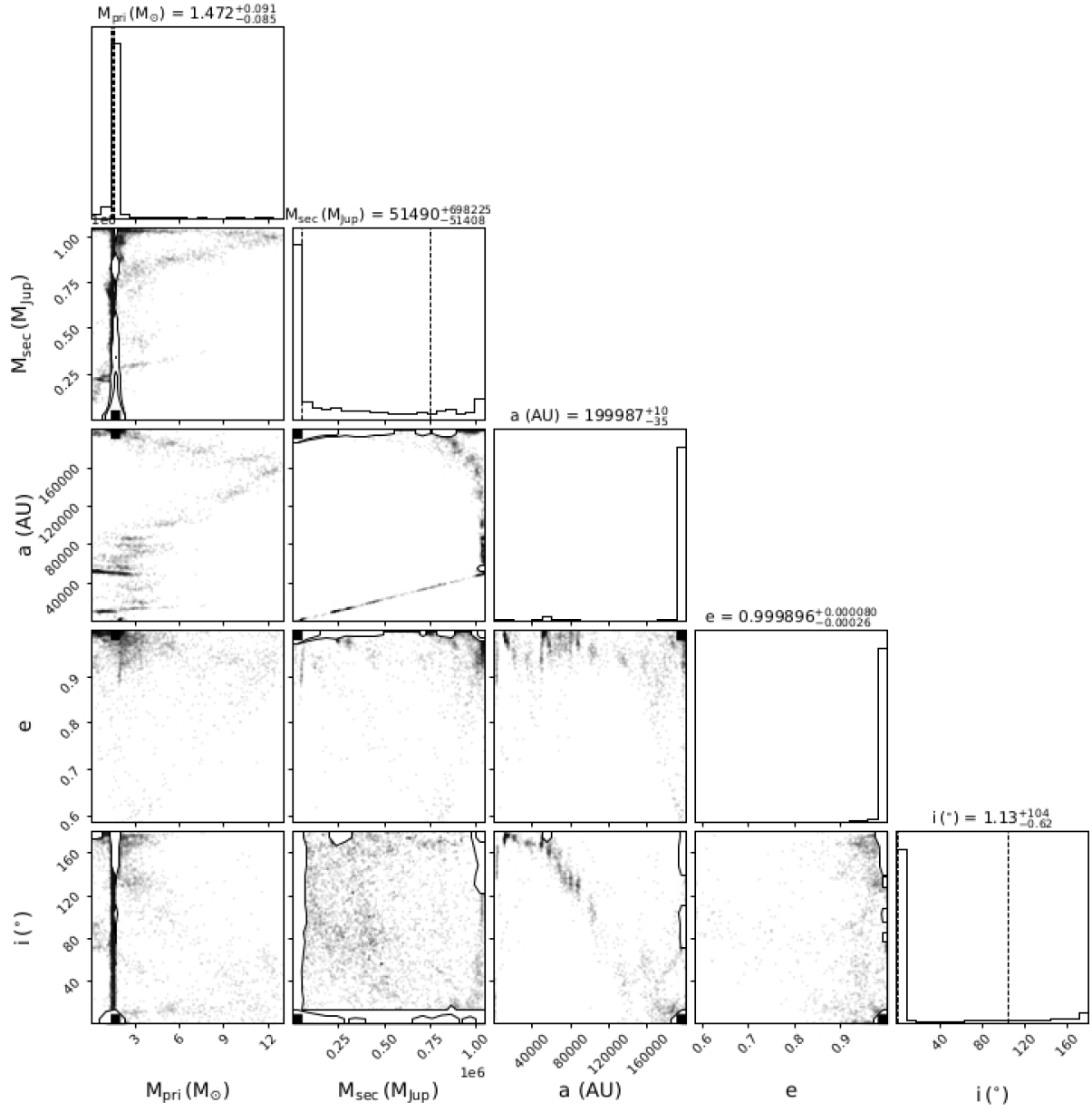

Figure A.9: correlation plot for HD 114082.

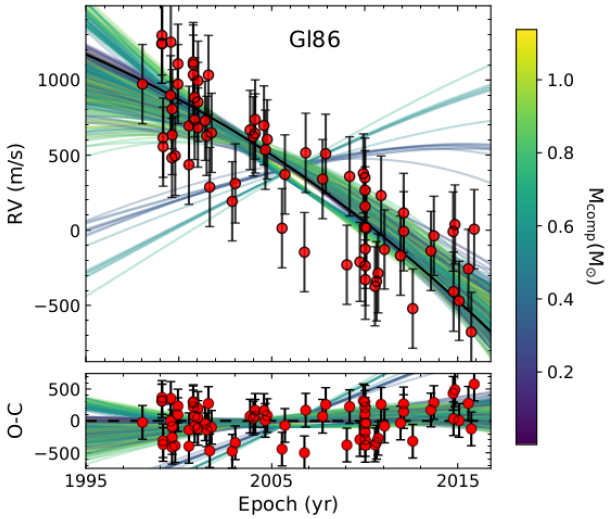

Figure A.10: The radial velocity plot for Gliese 86 with radial velocity as described in Zeng et al. (2022).

In the three sections below the plots for the rest of the systems are presented. Keep in mind that as stated in the discussion section, some plots are missing elements for unknown reasons.

A.1 AF Leporis plots

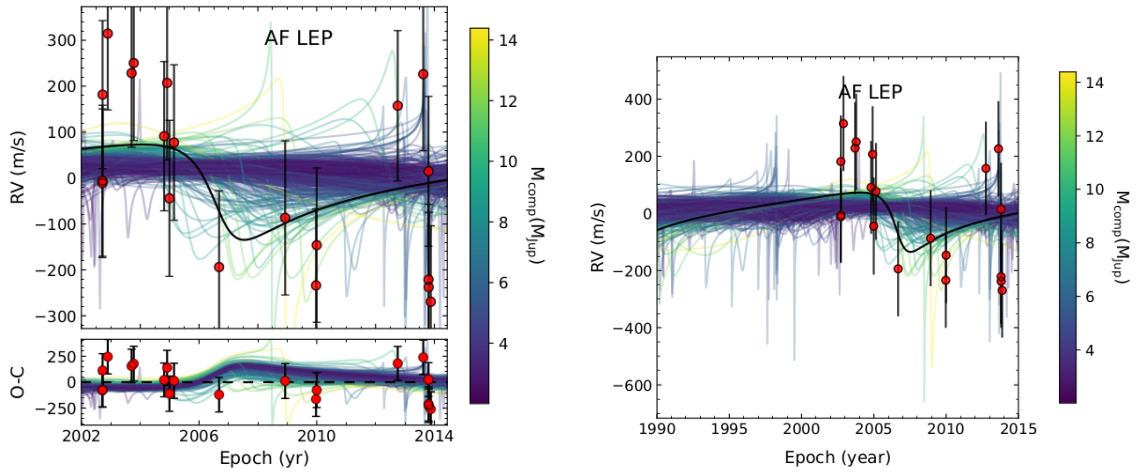

Figure A.11: The radial velocity plots for AF Leporis. The right and left plots are the same but with different levels of zoom.

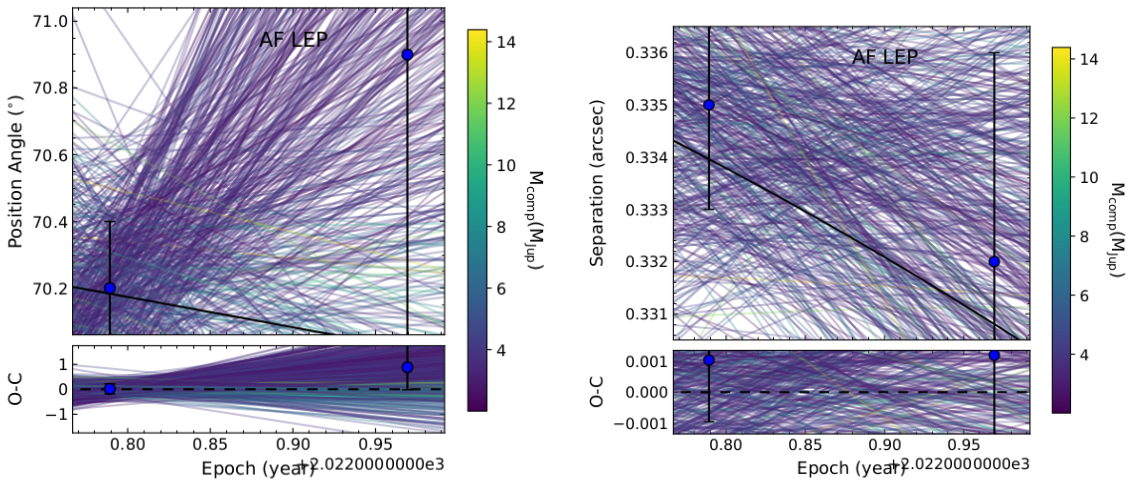

Figure A.12: Left: the position angle of AF Leporis relative its planet, right: the angular seperation of AF Leporis and its planet.

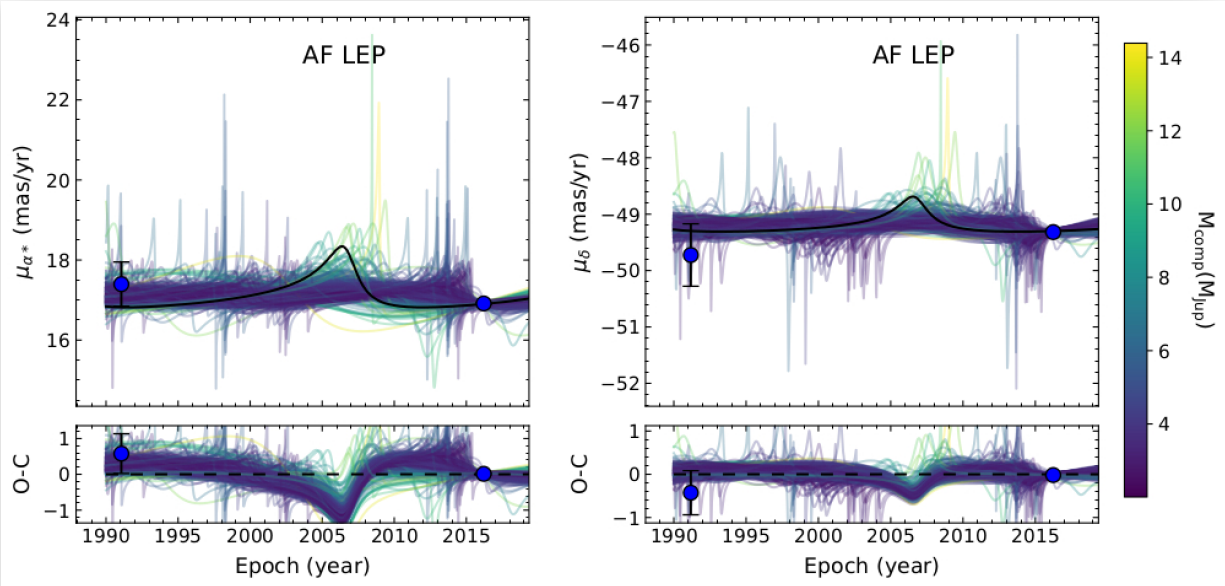

Figure A.13: The Hipparcos and Gaia proper motions. The left plot is the proper motion of AF Leporis and the right plot is the proper motion of the planet.

A.2 Gliese 105 (C) plots

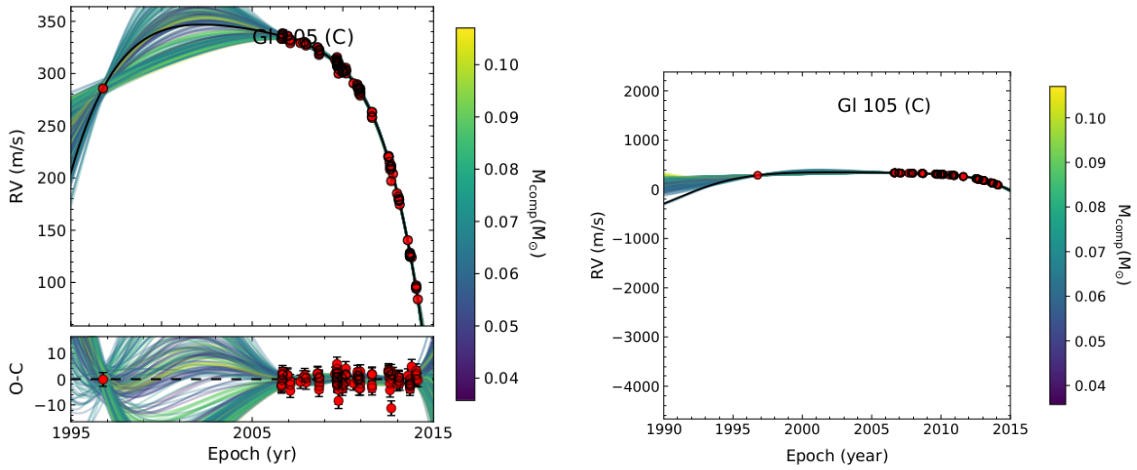

Figure A.14: The radial velocity plots for Gliese 105 A. The right and left plots are the same but with different levels of zoom.

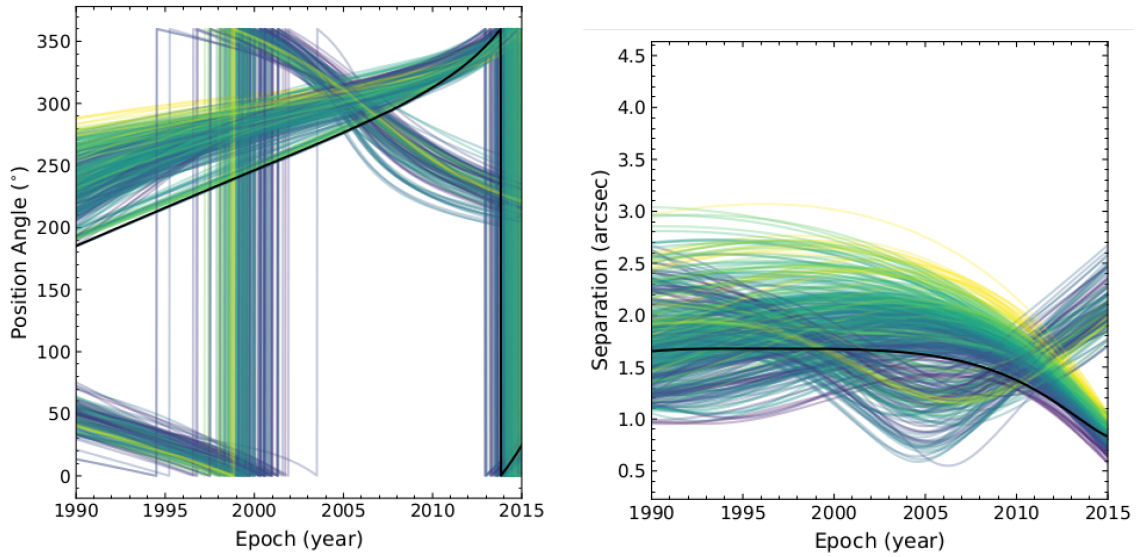

Figure A.15: Left: the position angle of Gliese 105 A-C, right: the angular separation between Gliese 105 A-C. These plots are missing the data points, the O-C plot and the color bar on the right side of the plot.

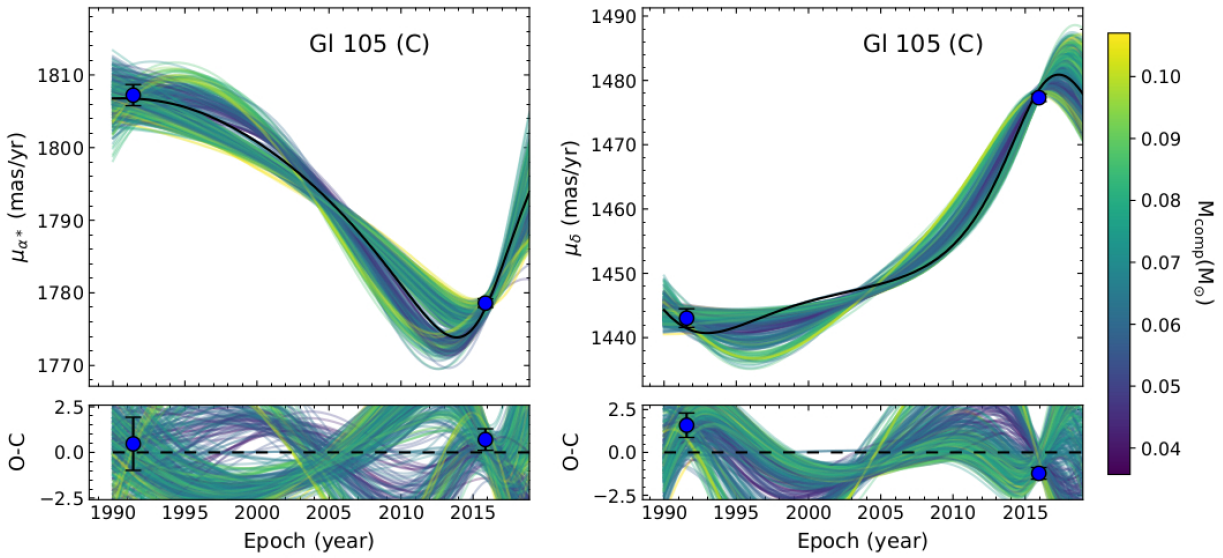

Figure A.16: The Hipparcos and Gaia proper motions. The left plot is the proper motion of Gliese 105 A and the right plot is the proper motion of Gliese 105 C.

A.3 Smethells 119 plots

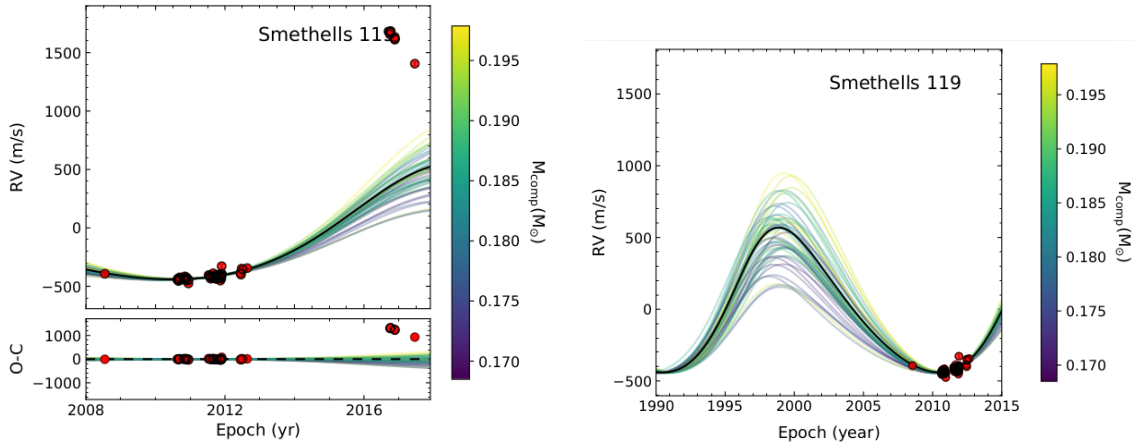

Figure A.17: The radial velocity plots for Smethells 119 A. The right and left plots are the same but with different levels of zoom.

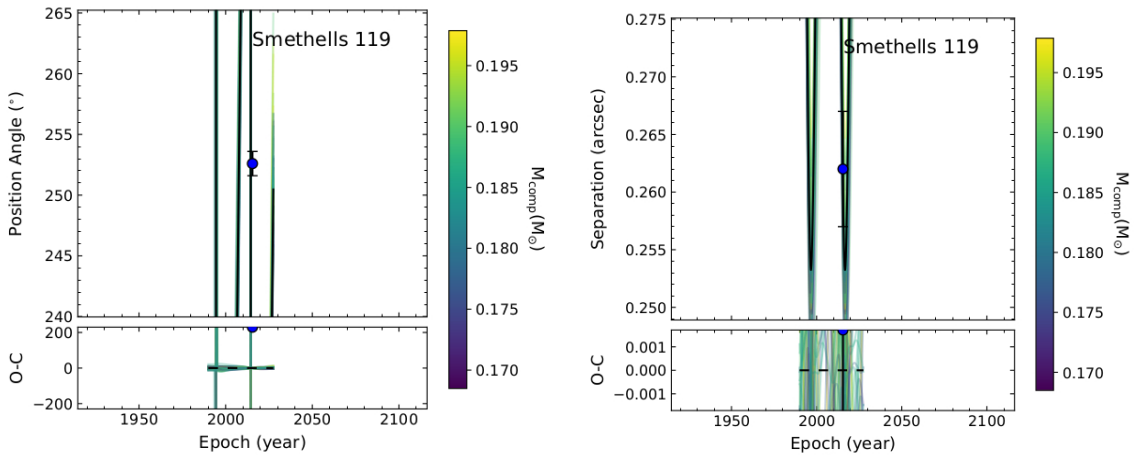

Figure A.18: Left: the position angle of Smethells 119 A-B, right: the angular separation between Smethells 119 A-B. The plots have an abnormal appearance since there is only one data point which makes it difficult to fit a trend to.

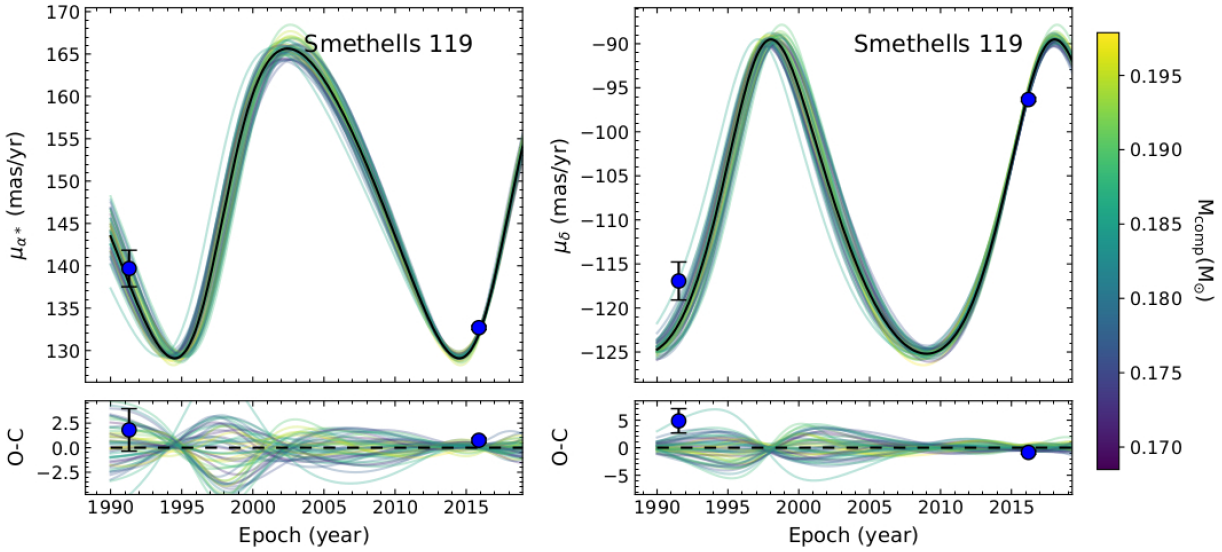

Figure A.19: The Hipparcos and Gaia proper motions. The left plot is the proper motion of Smethells 119 A and the right plot is the proper motion of Smethells 119 B.

A.4 HD 114082 plots

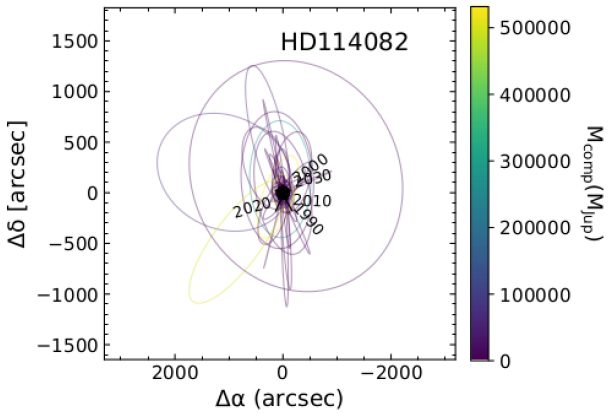

Figure A.20: Astrometric orbit plot of HD 114082

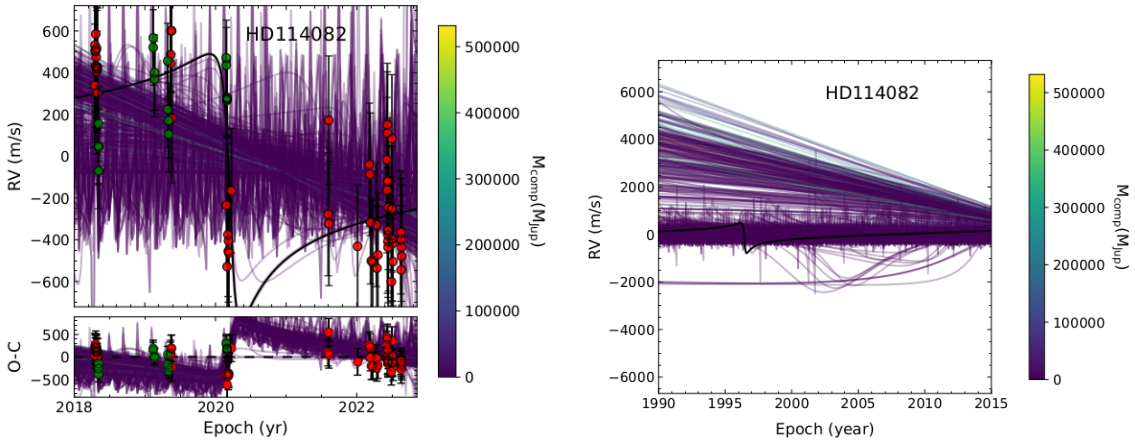

Figure A.21: The radial velocity plots for HD 114082. The right and left plots are the same but with different levels of zoom.

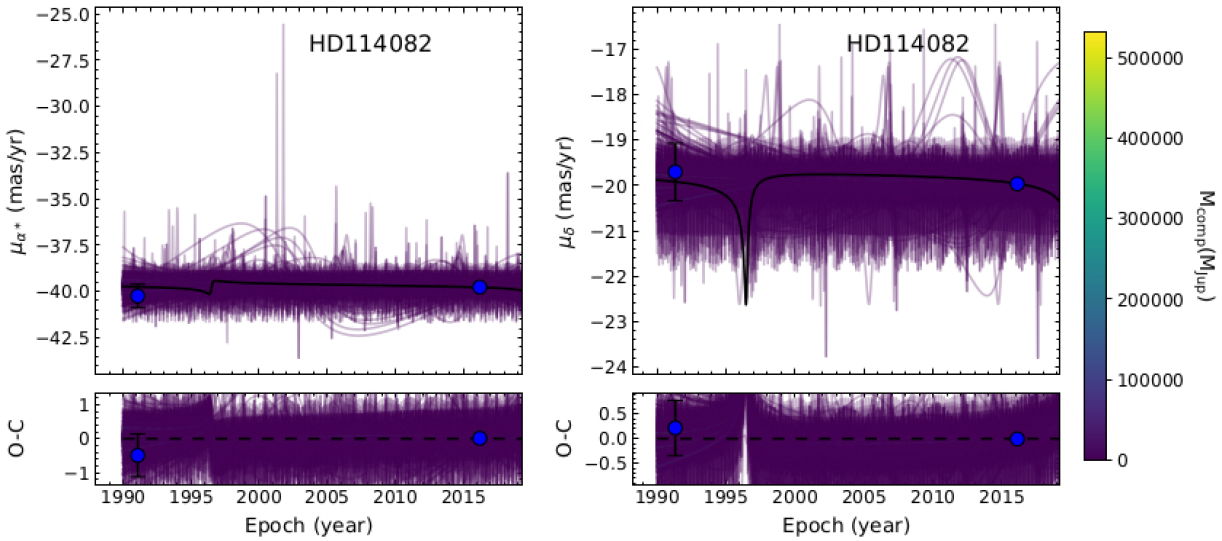

Figure A.22: The Hipparcos and Gaia proper motions. The left plot is the proper motion of HD 114082 and the right plot is the proper motion of the planet.

Appendix B

Tables

	Smethells 119	**Gl 86**	**Gl 105**	**AF Lep**
[MCMC settings]				
ntemps	10	10	10	10
nwalkers	100	100	100	100
nplanets	1	2	2	1
nstep	20000	20000	20000	20000
thin	50	50	50	50
nthreads	1	1	1	1
use_epoch_ astrometry	True	True	True	True
jit_per_inst	False	False	False	False
[priors serrings]				
mpri	0.8	0.8	0.74	1.2
mpri_sig	0.05	0.05	0.15	0.05
minjitter	1e-5	1e-5	1e-5	1e-5
maxjitter	1e3	1e3	1e3	1e3
[plotting]				
check_convergence	True	True	True	True
burnin	110	50	100	100
iplanet	0	0	1	0
start_epoch	1990	1990	1990	1990
end_epoch	2015	2015	2015	2015
num_orbits	50	50	500	500
num_steps	1500	1500	1500	1500
predicted_years	1990,2000, 2010, 2020,2030	1990,2000, 2010, 2020,2030	1990,2000, 2010, 2020,2030	1990,2000, 2010, 2020,2030
position_predict	2010	2020	2010	2010

Table B.1 continued from previous page

	Smethells 119	**Gl 86**	**Gl 105**	**AF Lep**
astrometry_ orbits_plot	True	True	True	True
astrometric_ prediction_plot	True	True	True	True
RV_orbits_plot	True	True	True	True
RV_plot	True	True	True	True
RV_instrument	All	All	All	All
relative_ seperation_plot	True	True	True	True
position_angle_plot	True	True	True	True
proper_motion_plot	True	True	True	True
proper_motion_ separate_plots	False	False	False	False
corner_plot	True	True	True	True
set_limit	False	False	False	False
xlim	1980, 2025	1980, 2025	1980, 2025	1980, 2025
ylim	-2.8, 2.8	-2.8, 2.8	-2.8, 2.8	-2.8, 2.8
marker_color	blue	blue	blue	blue
use_colorbar	True	True	True	True
colormap	viridis	viridis	viridis	viridis
reference	msec_solar	msec_solar	msec_solar	msec_jup
show_title	False	False	False	False
add_text	True	True	True	True
text_name	Smethells 119	Gl86	Gl 105 (C)	AF LEP
x_text	0.5	0.5	0.5	0.5
y_text	0.9	0.9	0.9	0.9
[**save results**]				
save_params	True	True	True	True
err_margin	0.16, 0.5, 0.84	0.16, 0.5, 0.84	0.16, 0.5, 0.84	0.16, 0.5, 0.84

Table B.1: Table of the settings in the configuration files for 4 systems. The setting that have been left out are the secondary Gaia variables since they are never used and all file path variables.